Engineering
Library

JUN 3 '47

Journal of Research

of the National Bureau of Standards

U S.

APRIL 1947

VOLUME 38 NUMBER 4

PERIODICALS OF THE NATIONAL BUREAU OF STANDARDS

Journal of Research

The National Bureau of Standards is the principal agency of the Federal Government for fundamental research in physics, chemistry, and engineering. It has the custody of the national standards of physical measurement in terms of which all working standards in research laboratories and industry are calibrated, and carries on necessary research leading to improvement in such standards and methods of measurement. It also has a general responsibility for basic research in physics, chemistry, and engineering, and for development of improved methods for testing materials and equipment. It determines physical constants and properties of materials, tests and calibrates standard measuring apparatus and reference standards, and studies technical processes. The results of the Bureau's research and investigations are published in the JOURNAL OF RESEARCH.

Research Papers

Reprints of individual articles appearing in the JOURNAL OF RESEARCH. They are made available to serve the needs of research workers, technical groups, and others for the separate papers relating to the special subjects in which they are interested.

Technical News Bulletin

Contains short but complete summaries of research, development, and testing in progress at the Bureau, accounts of the Bureau's national and international activities, scientific and technical announcements of new plans and programs, and a list of publications by members of the staff. It is a prompt and reliable source of official information of value to those who desire to keep in touch with the general activities of the Bureau.

Basic Radio Propagation Predictions

This is a monthly publication for those concerned with radio communication in determining the best sky-wave frequencies over any path at any time of day for average conditions for the month of prediction, which are made three months in advance. Charts of extraordinary-wave critical frequence for the F2 layer and of maximum usable frequency for a transmission distance of 4,000 km, of highest frequency of sporadic-E in excess of 15 Mc are included. In addition, there are various maps, charts, diagrams, and nomograms needed to make practical application of the world-contour charts, together with examples of their use.

ANNUAL SUBSCRIPTION Send order, with remittance, to Superintendent of Documents, U. S. Government Printing Office, Washington 25, D. C.	United States, Canada, Cuba, Mexico, Newfoundland, Republic of Panama	Other countries
JOURNAL OF RESEARCH of the National Bureau of Standards:		
12 monthly issues (2 volumes), paper covers	$4.50	$5.50
Bound volume (½ year, 1 volume), blue buckram	3.00	3.50
RESEARCH PAPERS	(*)	(*)
TECHNICAL NEWS BULLETIN, 12 monthly issues	1.00	1.35
BASIC RADIO PROPAGATION PREDICTIONS, 12 monthly issues	1.50	2.00

*The prices of the separate Research Papers appearing in this JOURNAL are given in the Contents. If 100 or more copies of any separate are ordered, a discount of 25 percent is allowed. Those who desire copies of separate Research Papers should send their orders and remittances without delay to the Superintendent of Documents, U. S. Government Printing Office, Washington 25, D. C. This will aid him to determine the number of copies to be printed for sale. Research Papers are not printed from electrotypes and usually no more reprints can be had when the first and only printing is exhausted.

Published with approval of Bureau of the Budget

U. S. DEPARTMENT OF COMMERCE
W. Averell Harriman, Secretary
NATIONAL BUREAU OF STANDARDS
E. U. Condon, Director

APRIL 1947
VOLUME • 38
NUMBER 4

JOURNAL OF RESEARCH

of the

NATIONAL BUREAU OF STANDARDS

Contents

RP		Page
1780.	Synchronization of oscillators. Robert D. Huntoon and Albert Weiss. (Price 10 cents)	397
1781.	Disintegration of scandium[46]. Irving Feister and Leon F. Curtiss. (Price 10 cents)	411
1782.	High-temperature X-ray diffraction apparatus. Alvin Van Valkenburg, Jr., and Howard F. McMurdie. (Price 10 cents)	415
1783.	Heats of combustion and isomerization of six nonanes. Walter H. Johnson, Edward J. Prosen, and Frederick D. Rossini. (Price 10 cents)	419
1784.	Structure of difructose anhydride II. Emma J. McDonald and Anne L. Turcotte. (Price 10 cents)	423
1785.	Mangabeira latex and rubber. Norman Bekkedahl and Waldemar Saffioti. (Price 10 cents)	427
1786.	Spectrographic determination of minor elements in portland cement. Armin W. Helz and Bourdon F. Scribner. (Price 10 cents)	439

For sale by the Superintendent of Documents, U. S. Government Printing Office, Washington 25, D. C. - Price 40 cents,
$4.50 per year on subscription

UNITED STATES GOVERNMENT PRINTING OFFICE, WASHINGTON : 1947

U. S. Department of Commerce
National Bureau of Standards

Research Paper RP1780
Volume 38, April 1947

Part of the Journal of Research of the National Bureau of Standards

Synchronization of Oscillators

By Robert D. Huntoon and Albert Weiss

A theory is presented which predicts the behavior of any self-limiting oscillator in the presence of an injected sinusoidal voltage or current of small but constant magnitude. The internal mechanism responsible for synchronization is not needed, and the theory is thus applicable to any source of alternating current. Experimental verification of the theory is presented for the case of a low-power Hartley oscillator operating at 11.5 megacycles.

The theory is extended to include the mutual synchronization of two oscillators of arbitrary properties, and a method of treating the mutual interaction of several oscillators is outlined.

The theory is applied to a number of examples to indicate briefly the properties of a synchronized oscillator when used as (1) a linear voltmeter for small voltages, (2) a field-intensity meter, (3) a linear amplitude modulation demodulator for small signals, (4) a frequency modulation demodulator, (5) a synchronous amplifier limiter. The use of a synchronized oscillator for these applications is of particular interest because microwave generators can be used in addition to the more conventional triode oscillators.

I. Introduction

The early experiments of Vincent,[1] followed by Appleton's[2] theoretical treatment, have led to a considerable interest in possible practical applications of the synchronization of oscillators.[3] Since the publication of these early papers there has been a continually growing literature on the subject,[4] with attention now primarily centered on (a) the use of an oscillator as a synchronous-amplifier-limiter for frequency modulation reception, and (b) the use of a chain of synchronous oscillators to drive a linear accelerator for the production of high-energy atomic particles. There are, of course, numerous other applications, some of which are discussed in terms of the theory that is the subject of this paper.

Following Appleton, theoretical treatments of oscillator synchronization have been concerned with the mechanism within a triode oscillator that accounts for synchronization. The phenomenon of synchronization with a disturbance impressed from an external source is not limited to triode oscillators. Rather, any source of alternating electromotive force whose frequency depends upon the load impedance attached to it (magnetron, for example) will exhibit similar behavior. It should thus be possible to discuss certain general features of synchronization without reference to the internal mechanism which accounts for it. The theory so derived will be generally applicable to all types of oscillators.

In a recent paper Adler[5] has developed a differential equation whose solution accounts for many of the observed phenomena of synchronization. Again, the triode oscillator mechanism has been the basis of the discussion. However, the scheme used by Adler can be extended in a manner

[1] J. H. Vincent, On some experiments in which two neighboring maintained oscillatory circuits affect a resonating circuit, Proc. Roy. Soc. (London) **32**, 84 (1920).

[2] E. V. Appleton, The automatic synchronization of triode oscillators, Proc. Cambridge Phil. Soc. **21**, 231 (1922).

[3] The term "oscillator" as used here means a source of harmonic vibration whose steady-state amplitude is limited to a finite value by some internal nonlinear characteristic.

[4] See, for example, Robert Adler, A study of locking phenomena in oscillators, Proc. Inst. Radio Engrs. **34**, 351 (1946).

[5] Robert Adler, A study of locking phenomena in oscillators, Proc. Inst. Radio Engrs. **34**, 351 (1946).

that does not involve the particular generator. The result is a differential equation similar to his but more general. In addition, amplitude behavior, as well as frequency behavior, can be included.

The development proceeds in a manner somewhat similar to Adler's and is based upon similar assumptions regarding time constants, etc. The performance of the oscillator is specified in terms of a set of compliance coefficients that show how amplitude and frequency depend upon the load impedance. The frequency coefficient is closely related to the conventional pulling parameter. The values of the coefficients are not derived here but are assumed to be given as constants of the problem. They may be derived theoretically or measured for the particular oscillator. Briefly, the scheme of the argument is that the given source of electromotive force is connected to a known load impedance [6] into which the outside disturbance is to be coupled. The frequency of oscillation F and some amplitude parameter A, such as d-c plate current, a-c plate swing, d-c grid bias, or output voltage are measured or calculated as a function of the load impedance. Each of the above parameters is expanded in a Taylor series about the operating value of the load impedance. Only first-order terms in the series are kept, so the theory is strictly true for small disturbances only. Actually, large disturbances are treated with reasonable accuracy.

The voltage (or current) coupled into the load impedance from the external source is treated as an added impedance (or admittance) in accordance with the compensation theorem.[7] This is valid if (1) the disturbance is so small that it does not materially alter the magnitudes of voltage or current established in the load by the oscillator, (2) both source and disturbance are free of harmonics, (3) both have the same frequency. The first limits the size of disturbance for which the theory is valid. The second does not ordinarily need consideration when circuit Q's are large. If harmonics are present to any great extent, a second-order theory will be needed. The third is avoided when the frequencies are not the same by saying that the impedance equivalent to the impressed disturbance varies with time in such a manner that its phase angle accounts for the difference frequency. This is a good enough approximation when the conditions established by Adler are met, i. e., when the difference frequency is small compared with the band width of the circuits involved.

By using the compliance coefficients and the impedance equivalent to an impressed disturbance, the general properties of synchronization can be deduced.

II. Synchronization by an Impressed Voltage

In the discussion to follow, complex quantities will be represented by bold-faced type; quantities not so designated will denote absolute magnitudes. The factor $e^{j\omega t}$ will usually be omitted.

1. Compliance Coefficients

Let figure 1 represent an energy source of the type that converts d-c energy to a-c energy, such as a typical triode oscillator or magnetron.

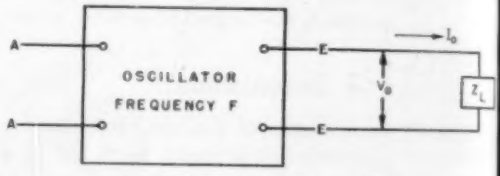

FIGURE 1.—*Self-limiting oscillator.*

For the discussion, we are interested in two pairs of terminals. The terminals marked E are assumed to be the output terminals of the device for delivering a-c power to a load impedance Z_L or admittance Y_L.

Terminals marked A represent a pair of terminals that give a d-c or a-c indication of the amplitude of oscillation, such as grid bias, d-c plate current, or the reading of a diode voltmeter across the output circuit.

Assume that there are also available, if necessary, instruments which indicate either the voltage V_0 across the load or current I_0 through it.

Let $\boldsymbol{V}_0$ and $\boldsymbol{I}_0$ be the initial or undisturbed value of these quantities when the oscillator is feeding its load circuit. Similarly, let F represent the frequency of the oscillator, and F_0 its undisturbed value.

[6] This load impedance may be a part of the oscillator circuit, such as the plate tank of a triode oscillator.

[7] F. E. Terman, Radio Engineers Handbook, p. 198 (McGraw-Hill Book Co., Inc., New York, N. Y., 1943).

We proceed to evaluate the performance of the oscillator by adding small impedances, z, in series with the load. We determine the oscillator performance by measuring the effect of z as shown by changes in the reading across A–A. Suppose that the information is presented in the form of a d-c voltage, A, between terminals A–A, grid bias, for example. The useful parameters of the oscillator will be specified by the following compliance coefficients:

$$A_r=\left.\frac{\partial A}{\partial r}\right|_{r=0} \qquad A_x=-\left.\frac{\partial A}{\partial x}\right|_{x=0} \tag{1}$$

$$F_r=\left.\frac{\partial F}{\partial r}\right|_{r=0} \qquad F_x=-\left.\frac{\partial F}{\partial x}\right|_{x=0}, \tag{2}$$

where

$$z=r+jx. \tag{3}$$

As already indicated, we proceed by expanding A and F in a Taylor expansion about A_0 and F_0, keeping only first-order terms. This gives

$$A-A_0=rA_r-xA_x \tag{4}$$

$$F-F_0=rF_r-xF_x. \tag{5}$$

There will also be occasion to use two complex compliance coefficients, an amplitude coefficient, C_A, and a frequency coefficient, C_F. They are defined by

$$C_A=C_Ae^{+j\alpha}=A_r+jA_x=\sqrt{A_r^2+A_x^2}e^{+j\alpha} \tag{6}$$

$$C_F=C_Fe^{+j\beta}=F_r+jF_x=\sqrt{F_r^2+F_x^2}e^{+j\beta}. \tag{7}$$

Throughout the discussion only series impedance will be used; the argument can be based upon admittances in a similar manner.

2. Synchronization Equation

Suppose that a small voltage is induced in the load circuit from an outside source. Assume the voltage is small enough so that the change in I can be neglected, and that we can, with sufficient accuracy, represent I by its initial value I_0. By the compensation theorem we can replace the induced voltage v by a small impedance z, where

$$z=\frac{v}{I_0}e^{j\phi}. \tag{8}$$

We may thus write (keeping only real parts)

$$A-A_0=C_Az=\frac{C_Av}{I_0}\cos(\phi+\alpha) \tag{9}$$

$$F-F_0=C_Fz=\frac{C_Fv}{I_0}\cos(\phi+\beta), \tag{10}$$

where

$$\tan\alpha=\frac{A_x}{A_r}$$

$$\tan\beta=\frac{F_x}{F_r}, \tag{11}$$

and it will be remembered that in typical oscillators $A_x \ll A_r$, while $F_r \ll F_x$. Thus α is usually very small, and β is nearly $\pi/2$. There is, however, a special, interesting case where this is not true. It will be discussed later.

We now proceed with eq. 10, as done by Adler, to establish the synchronization equation. Assume that the injected voltage v has the frequency F^1 and that the instantaneous frequency of the oscillator is F. We then have

$$\frac{1}{2\pi}\frac{d\phi}{dt}=F^1-F=(F^1-F_0)-(F-F_0). \tag{12}$$

If F^1-F is not too large, we can consider the equivalent impedance z to be varying with time as its phase angle changes. If the frequency changes are not too rapid,[8] the oscillator frequency will follow the impedance changes in the manner predicted by eq. 10. We may thus write

$$\frac{1}{2\pi}\frac{d\phi}{dt}=F^1-F_0-\frac{C_Fv}{I_0}\cos(\phi+\beta), \tag{13}$$

an equation similar to that obtained by Adler. F^1 and F_0 are constant frequencies, the latter being the free-running frequency of the oscillator. Equation 13 is a differential equation for ϕ, and its solution shows how the beat frequency $(1/2\pi)(d\phi/dt)$, varies with time.

[8] See remarks by Robert Adler, A study of locking phenomena in oscillators, Proc. Inst. Radio Engineers **34**, 351 (1946). Also note:

$$I=Ie^{j2\pi Ft}$$

$$v=ve^{j2\pi F^1t}$$

$$z=\frac{v}{I}e^{j2\pi(F^1-F)t}=\frac{v}{I}e^{j\phi}$$

If we let

$$F_1 - F_0 = f$$

and

$$\frac{C_p v}{I_0} = Kv, \tag{14}$$

eq. 13 becomes

$$\frac{1}{2\pi}\frac{d\phi}{dt} = f - Kv\cos(\phi+\beta). \tag{15}$$

This makes f the beat frequency that would exist if the oscillator did not react to the injected voltage, i. e., the undisturbed beat frequency.

It is evident immediately from eq 15 that the solution $\phi(t)$ is of a complicated periodic form when

$$f^2 > K^2v^2 \tag{16}$$

and reduces exponentially to a steady value of ϕ when

$$f^2 < K^2v^2. \tag{17}$$

Equation 17 corresponds to synchronization between the injected voltage and the oscillator current at a fixed phase angle, ϕ. As we are interested primarily in synchronization, the solution of eq 15, subject to eq 17, is needed. It is

$$\frac{\cos\psi - \cos(\phi+\beta)}{1-\cos(\phi+\beta-\psi)} = \text{const}\; e^{-2\pi f\sqrt{K^2v^2-f^2}}, \tag{18}$$

where

$$\cos\psi = \frac{f}{Kv}, \tag{19}$$

from which we observe that the steady state value of ϕ for large t is given by

$$\cos(\phi+\beta) = \frac{f}{Kv}. \tag{20}$$

The equilibrium value is approached in such a manner that the time constant is approximately

$$\tau \cong \frac{1}{2\pi\sqrt{K^2v^2-f^2}} = \frac{1}{2\pi Kv\sin\psi}. \tag{21}$$

There are two values of $(\phi+\beta)$ that satisfy eq 20. One corresponds to stable equilibrium, the other to unstable equilibrium. From eq 15

$$\frac{1}{2\pi}\frac{d}{a\phi}\left(\frac{d\phi}{dt}\right) = Kv\sin(\phi+\beta). \tag{15a}$$

For stability $(d/d\phi)(d\phi/dt)$ must be negative Thus only values of $(\phi+\beta)$ such that sin $(\phi+\beta)$ is negative lead to stable synchronization.

Equation 20 differs from the result obtained by Adler in the phase angle β. The size of β is important where the exact phase of lock-in is important, as in the application to the linear accelerator.

Equation 20 shows that synchronization can be obtained over a range of f, such that

$$-Kv < f < Kv,$$

or over a band of frequencies

$$\Delta f = 2Kv. \tag{22}$$

3. Amplitude changes

The quantity $a = A - A_0$ expresses the change of some convenient amplitude parameter, such as radio-frequency voltage, d-c grid bias, or d-c plate current, in the presence of the injected signal. It is evident from eq 10 that a and f are functionally related through the parameter ϕ. As f is varied from one edge of the synchronization band to the other, ϕ varies through the range

$$-\beta > \phi > -\pi - \beta. \tag{23}$$

This variation in ϕ produces variations in a, so that it exhibits a characteristic wave from which $(\alpha-\beta)$ can be readily deduced. By defining new quantities,

$$\begin{aligned}\delta &= (\phi+\beta)\\ \rho &= (\alpha-\beta).\end{aligned} \tag{24}$$

we can write eq 10 in terms of the dimensionless variables (U, W)

$$U = \frac{fI_0}{C_p v} = \cos\delta \tag{25}$$

$$W = \frac{aI_0}{C_A v} = \cos(\delta+\rho), \tag{26}$$

from which it is evident that the form of the a versus f wave is independent of I_0 and v (for small disturbances). Also the relation between U and W is an ellipse which degenerates into a line when $\rho = 0$ or π, and into a circle when $\rho = \pm\pi/2$.

Figure 2 shows the form of the synchronization amplitude pulse in terms of the variables U and W for several values of ρ. A study of figure 2 and eq 25 and 26 shows the following:

1. When $\rho = \pm\pi/2$, a is zero at the ends of the synchronization band, and the a-curve is symmetrical.

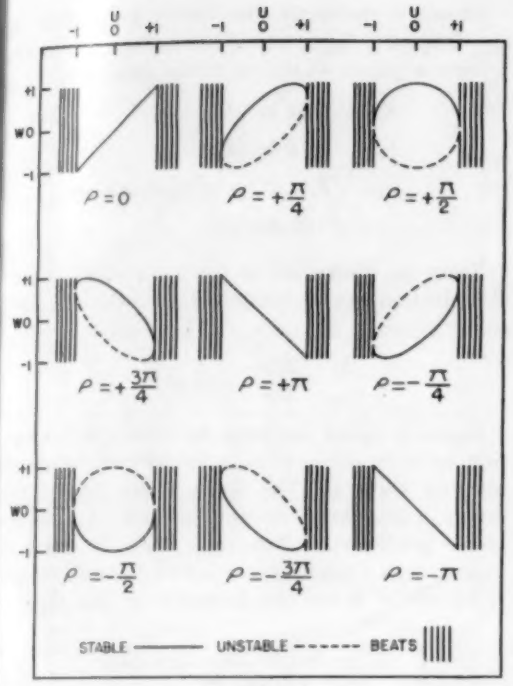

FIGURE 2.—*Forms of the U-W curve in the region of synchronization.*

2. When $\rho \neq \pm\pi/2$, the a-wave is not symmetrical, and a is not zero at the edge of the synchronization band. Thus at the instant beats cease, the phase between the oscillator and the injected voltage is such that there is a resistance component of loading and a has a finite value.

3. When $\rho = 0$ or π, there is a linear relation a and f. The a-curve is completely asymmetric and a has its largest value at the edge of the synchronization band.

4. The maximum value of a is the same for all curves, and has the value

$$a_{max} = \frac{C_A v}{I_0}. \tag{27}$$

5. At the high-frequency edge of the synchronization band

$$a = a_{max} \cos \rho. \tag{28}$$

By using this relation, ρ can be determined directly from the a-curve as well as by measurement of the compliance coefficients.

6. Equations 25 and 26 show that the phase between injected voltage and undisturbed current is $\pm\beta$ at the edge of the synchronization band. For a simple oscillator circuit β is usually nearly $\pi/2$.

7. From eq 22, 25, and 26 we see that

$$\frac{\Delta f}{a_{max}} = \frac{2C_F}{C_A}, \tag{29}$$

which shows that the synchronization band width per volt injected is a constant. As a is proportional to v, it is often convenient to use a directly as a measure of v without bothering to measure v. This obviates the need for knowledge of I_0 as the synchronization band can be predicted directly from eq 29, as is done in section III.

III. Experimental measurements

In order to check the foregoing theory, experimental measurements were made on a small Hartley oscillator operating at 11.5 megacycles Radio frequency voltage for injection was supplied by a push-pull power oscillator operating at 10 times the plate voltage of the small oscillator and very loosely coupled to it inductively. Frequencies were read on a receiver arranged with panoramic adapter and vernier-vernier tuning control. Any pulling of the power oscillator by the small oscillator is thus removed from the frequency readings. As will be seen in section IV, the pulling of the driving oscillator does play a part in the observed bank of synchronization, and the power level of this oscillator must be kept as high as practicable.

Figure 3 is a circuit diagram of the test oscillator showing the method of voltage injection and a

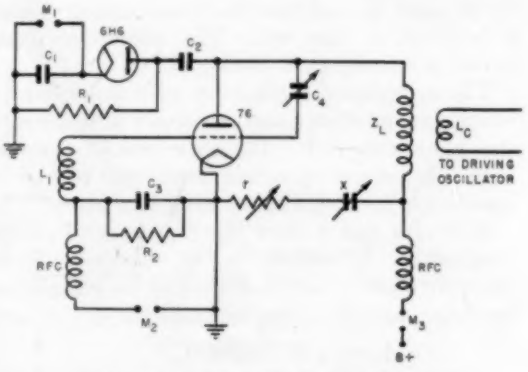

FIGURE 3.—*Circuit of test oscillator.*

Z_{L_1} 3.9 μh; L_2, 5.5 μh; L_C, coupling coil; C_1, 0.001 μf; C_2, 0.001 μf; C_3, 0.00007 μf; C_4, 0.00002 μf; R_1, 1.0 megohm; R_2, 15,000 ohms; M_1, meter to indicate radio-frequency plate voltage; M_2, grid-voltage meter; M_3, plate-current meter; r, series resistance; x, series reactance; RFC, 2.5 mh.

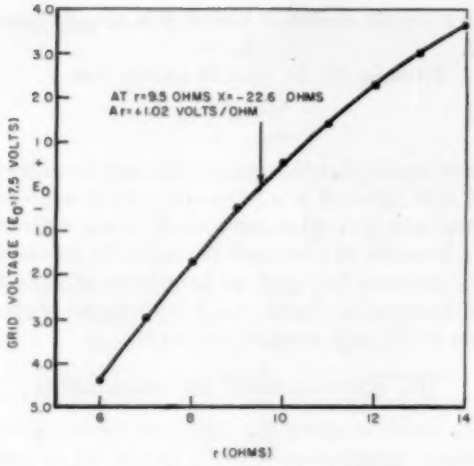

FIGURE 4.—*Experimental curve for evaluation of A_r.*

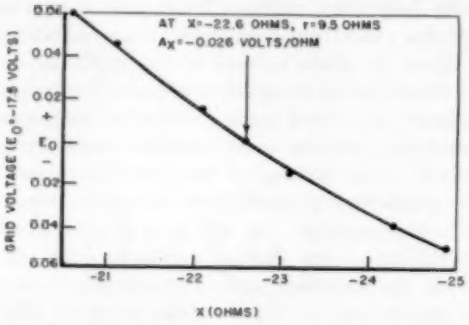

FIGURE 5.—*Experimental curve for determination of A_x.*

diode for measuring radio frequency plate swing. It will be noted that the plate coil has been used for the load, Z_L, and that the synchronizing voltage is injected in this coil. The additional diode circuit is referred to in section IV.

The compliance coefficients were measured by inserting capacitors x and resistors r in series with the plate-tank coil. To allow measurement on both sides of the operating point, this point was specified to be $r=9.5$ ohms, $x=-22.6$ ohms.

Figures 4 and 5 show the experimental curves from which A_r and A_x can be obtained. From them we observe that the value of the compliance coefficients at the operating point are

$$A_r=+1.02 \text{ v/ohm}$$

$$A_x=-0.026 \text{ v/ohm}$$

$$C_A=\sqrt{A_r^2+A_x^2}=1.02 \text{ v/ohm}$$

$$\alpha=-1.5 \text{ degrees.}$$

Figure 6 shows similar curves for evaluating the frequency compliance parameters. The appropriate values at the operating point are

$$F_r=-2.74 \text{ kc/ohm}$$

$$F_x=+10.5 \text{ kc/ohm}$$

$$C_F=\sqrt{F_r^2+F_x^2}=10.8 \text{ kc/ohm}$$

$$\beta=+105 \text{ degrees.}$$

From the above values the band width of synchronization can be computed. Substitution into eq. 29 gives

$$\frac{\Delta f}{a_{max}}=\frac{2C_F}{C_A}=21.2 \text{ kc/v.}$$

Figure 7 shows the band width of synchronization as a function of a_{max} for several values of injected voltage. The slope of the line at the origin is 20.5 kc/v, in good agreement with the above prediction. Note also that the curve is linear over a considerable range of injected voltage.

To check upon the linearity of the relation

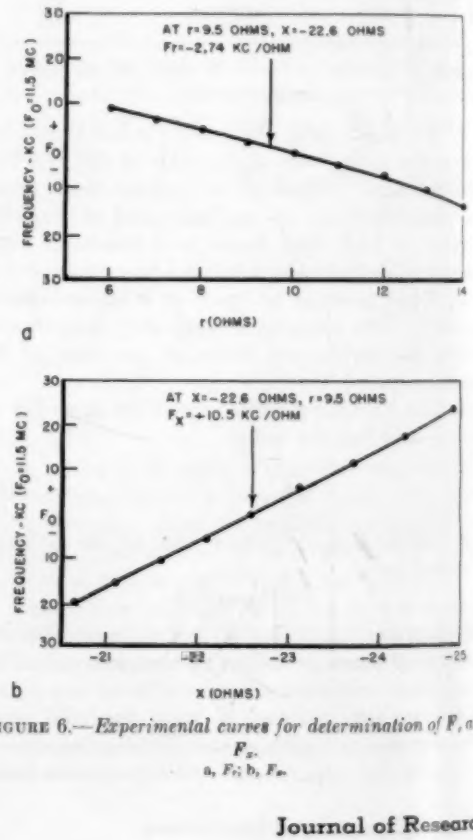

FIGURE 6.—*Experimental curves for determination of F_r and F_x.*
a, F_r; b, F_x.

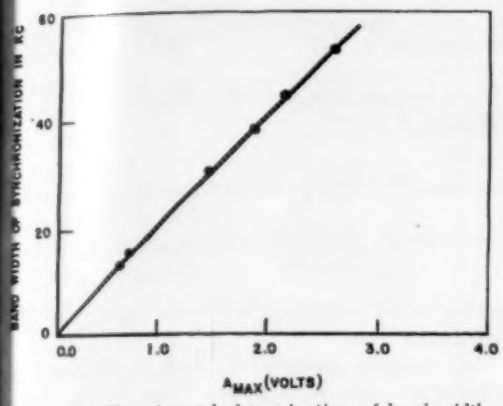

FIGURE 7.—*Experimental determinction of band width of synchronization in terms of injected voltage as measured by* a_{max}. *Slope of the curve 20.5 kc/v.*

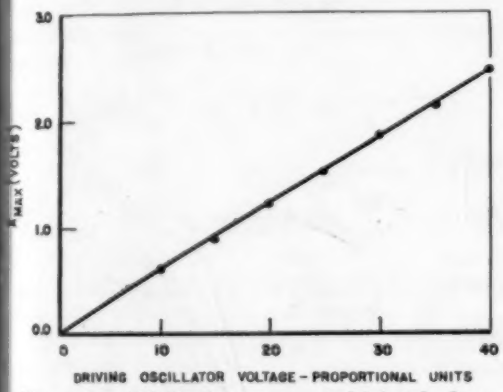

FIGURE 8.— *Relation between* a_{max} *and injected voltage.*

between a_{max} and v, a_{max} was measured as a function of v. The power-oscillator voltage was measured by a diode to give a number proportional to v; v was not measured directly. Figure 8 shows the result. Note that a is proportional to v over a surprisingly large range of values. The observed linearity of a_{max} as a function of v implies that f is also linear in v, as f was linear in a_{max}.

The theory also predicts that the curve of U versus W for this oscillator should be very nearly a semicircle. Figure 9, a, shows the measured U versus W curve. The solid curve is the theoretical one for $\rho=(-106.5°)$. Solid dots represent experimental values obtained by sweeping the power oscillator from high to low frequency through the synchronization band. Crosses represent the data when the frequency is swept in the reverse direction. There is no noticeable evidence of any hysteresis effect here. The simple theory would not indicate that there should be any, but there is some mention of such an effect in Appleton's papers.

The curve was also run for a large injected signal. The result is shown by circles and triangles in figure 9, b. The large signal gives poorer fit, but there is no evidence of hysteresis.

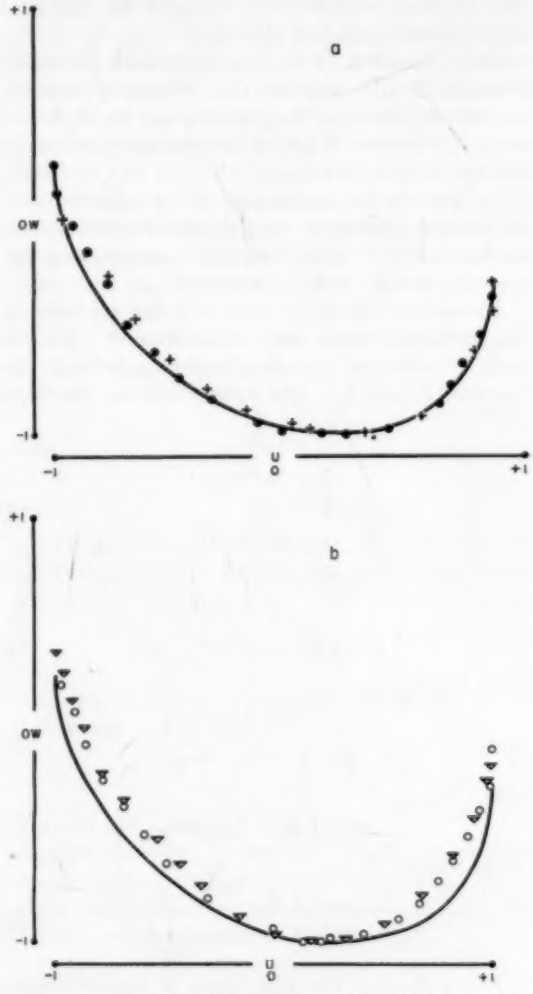

FIGURE 9.—*Experimental and theoretical U-W curves for the test oscillator.*

a, Solid line, theoretical curve for $\rho=(-106.5°)$; solid dots, experimental values sweeping from high to low frequency; crosses, experimental values sweeping from low to high frequency; $a_{max}=0.92$ v; b, experimental and theoretical U-W curves for the test oscillator. Solid line, theoretical curve for $\rho=(-106.5°)$; circles, experimental values sweeping from high to low frequency; triangles, experimental values, sweeping from low to high frequency; $a_{max}=4.9$ v.

IV. Mutual Synchronization of Oscillators

Consider two oscillators of the form shown in figure 1, and let them be coupled by a mutual impedance

$$\boldsymbol{Z}_{12}=Z_{12}e^{j\phi_{12}}.$$

Let the two systems be identified by subscripts 1 and 2. The coupling should be so arranged that the coupled voltages are induced in the load impedances $\boldsymbol{Z}_L$ of each system.

Both Z_{12} and ϕ_{12} will, in general, be functions of frequency. To simplify the present discussion, we assume that this dependence can be neglected over the narrow range of frequencies covered by the synchronization band.

As we are interested only in synchronization, we assume that both oscillators are synchronized at frequency F, and that their undisturbed frequencies are F_{01} and F_{02}, respectively.

In order to specify phases, we refer all phases to the current $\boldsymbol{I}_1$ in the load of oscillator 1. We will seek the value of the phase angle θ_{12} between the currents $\boldsymbol{I}_1$ and $\boldsymbol{I}_2$. We write (omitting the term $e^{j2\pi Ft}$)

$$\left.\begin{aligned}\boldsymbol{I}_1&=I_1e^{j0}\\ \boldsymbol{I}_2&=I_2e^{j\theta_{12}}\\ \boldsymbol{V}_1&=v_1e^{j\phi_1}\\ \boldsymbol{v}_2&=v_2e^{j(\theta_{12}+\phi_2)}\\ \boldsymbol{Z}_{12}&=Z_{12}e^{j\phi_{12}}\end{aligned}\right\}\tag{30}$$

Now,

$$\boldsymbol{v}_1=\boldsymbol{I}_2\boldsymbol{Z}_{12}=I_2Z_{12}e^{j(\theta_{12}+\phi_{12})},\tag{31}$$

from which

$$\left.\begin{aligned}v_1&=I_2Z_{12}\\ \theta_{12}+\phi_{12}&=\phi_1+2n\pi,\end{aligned}\right\}\tag{32}$$

also

$$\boldsymbol{v}_2=\boldsymbol{I}_1\boldsymbol{Z}_{12}=I_1Z_{12}e^{j\phi_{12}},\tag{33}$$

from which

$$\left.\begin{aligned}v_2&=I_1Z_{12}\\ \phi_{12}&=\theta_{12}+\phi_2+2n\pi\end{aligned}\right\}\tag{34}$$

We will drop the $2n\pi$, since it has no further interest.

Each of the oscillators will react to the coupled voltage independently of the other oscillator. Thus we write two equations like eq 10 and get

$$F-F_{10}=\frac{C_{F1}v_1}{I_{01}}\cos(\phi_1+\beta_1)\tag{35}$$

$$F-F_{20}=\frac{C_{F2}v_2}{I_{02}}\cos(\phi_2+\beta_2).\tag{36}$$

These we can combine with the aid of eq 31, 32, 33, and 34 to get

$$F_{20}-F_{10}=\frac{C_{F1}v_1}{I_{01}}\left[\cos(\theta_{12}+\phi_{12}+\beta_1)-\frac{C_{F2}}{C_{F1}}\left(\frac{I_{01}}{I_{02}}\right)^2\cos(-\theta_{12}+\phi_{12}+\beta_2)\right],\tag{37}$$

which is an equation involving θ_{12} as the only unknown.

We observe immediately from eq 37 that both oscillators contribute to the band width of synchronization. To see the effect more clearly we write

$$\left.\begin{aligned}\Phi&=(\theta_{12}+\phi_{12}+\beta_1)\\ \epsilon_1&=(-\beta_2-\beta_1-2\phi_{12})\\ k&=\frac{C_{F2}}{C_{F1}}\left(\frac{I_{01}}{I_{02}}\right)^2\end{aligned}\right\}\tag{38}$$

and get

$$F_{20}-F_{10}=\frac{C_{F1}v^1}{I_{01}}[\cos\Phi-k\cos(\Phi+\epsilon_1)]\tag{39}$$

$$=\frac{C_{F1}v_1}{I_{01}}[\sqrt{1+k^2-2k\cos\epsilon_1}\cos(\Phi+\epsilon_2)]\tag{40}$$

where

$$\tan\epsilon_2=\frac{-k\sin\epsilon_1}{1-k\cos\epsilon_1}.$$

From eq 40 we see that the two oscillators synchronize over a band of frequencies Δf_{12} given by

$$\Delta f_{12}=\Delta f_1\sqrt{1+k^2-2k\cos\epsilon_1}.\tag{41}$$

If oscillator 2 is much more powerful than oscillator 1 and otherwise identical, k will be very small and Δf_{12} becomes equal to Δf_1.

From this it can be seen that is is important to have the driving oscillator more powerful than the test oscillator when making synchronization measurements. If the two are identical, k will be 1, and the band of synchronization can vary from 0 to $2\Delta f_1$, depending on ϵ_1.

The allowed values of Φ, and hence of θ, can be obtained from eq 37, 38, 39, and 40 when the necessary parameters are given.

The problem of N oscillators can be set up in a manner similar to that for two oscillators. We proceed to indicate the operations required. Let the oscillators be indicated by subscripts 1 to N, and assume them to be synchronized. As before, we seek the $N-1$ phase angles $\theta_{12} \ldots \theta_{1N}$ relating the phase of the current in the tank of each oscillator to that in oscillator 1.

The mutual-impedances coupling the oscillators will be specified by

$$\mathbf{Z}_{xy}=Z_{xy}e^{j\phi_{xy}}. \tag{42}$$

There are the additional relations

$$\mathbf{I}_1=I_1e^{j0};\ \mathbf{I}_2=I_2e^{j\phi_{12}} \ldots \mathbf{I}_N=I_Ne^{j\phi_{1N}} \tag{43}$$

$$\mathbf{v}_1=v_1e^{j\phi_1} \ldots \mathbf{v}_N=v_NE_N^{j\phi} \tag{44}$$

and the system of equations expressing the interaction

$$\begin{aligned}
\mathbf{v}_1&=Z_{12}I_2e^{j(\phi_{12}+\theta_{12})} \ldots Z_{1N}I_Ne^{j(\phi_{1N}+\theta_{1N})} \\
&\vdots \\
\mathbf{v}_N&=Z_{1N}I_1e^{j(\phi_{1N})} \ldots Z_{N(N-1)}I_{N-1}e^{j(\phi_{N(N-1)}+\theta_{1(N-1)})}
\end{aligned} \tag{45}$$

Note that all the diagonal elements in eq 45 are missing. These can be omitted as it is assumed that the I's are given and are not appreciably disturbed by the coupled voltages v_N.

By equating members of eq 45 with corresponding members of eq 44, we get N equations that are to be solved for the $N\phi_N$ in terms of $\theta_{12} \ldots \theta_{1N}$ and the ϕ_{xy}.

We can now write the N equations of synchronization

$$\left.\begin{aligned}
F-F_{01}&=\frac{C_{F1}v_1}{I_{01}}\cos(\phi_1+\beta_1) \\
&\vdots \\
F-F_{0N}&=\frac{C_{FN}v_N}{I_{0N}}\cos(\phi_N+\beta_N).
\end{aligned}\right\} \tag{46}$$

The ϕ_N are known from the solution of eq 45 as functions of ϕ_{xy} and θ_{1N}; the C_F's and I_{N0}'s are specified. We substitute for $\phi_1 \ldots \phi_N$ their values in terms of the ϕ_{xy} and the $N-1$ quantities θ_{1N}. Then results a system of N equations to be solved for the $N-1$ quantities $\theta_{12} \ldots \theta_{1N}$ and F. Solution of eq 46 completes the problem.

V. Applications

Several interesting applications of the synchronized oscillator, some of which have been described elsewhere, can be studied with the aid of this theory. In what follows no attempt has been made to make an exhaustive study of any particular application but rather to indicate as a basis for further investigation some interesting applications of the synchronized oscillator.

1. Linear Radio-Frequency Voltmeter

From eq 27 and the argument which led to it, it can be seen that a_{max} is proportional to the injected voltage v. Moreover, it has been shown that the value of a_{max} does not depend upon C_F, α, or β. Thus the properties of the device as a voltmeter can be determined by a substitution of resistors and condensers in its load circuit where the voltage to be measured is injected. The indication of voltage can be obtained from the dc grid bias, or dc plate current or from a diode that reads the radio-frequency voltage across some part of the circuit.

If V is the radio-frequency voltage (peak) on the load impedance Z_L, then

$$V=I_0Z_L,$$

and

$$a_{max}=C_AZ_L\frac{v}{V}. \tag{47}$$

Typical values measured on the experimental oscillator are $C_A=+1.02$ v/ohms; $Z_L=236$ ohms; $V=47.0$ v. From which

$$v=\frac{a_{max}}{5.1}. \tag{48}$$

If the oscillator is running stably, it will be found very nearly that

$$C_A=SV, \tag{49}$$

where S is a constant of the oscillator. Figure 10 shows a curve of C_A versus V, which demonstrates the approximately linear dependence of C_A on V. S has the dimensions of a conductance and has the value 0.02 mho for the oscillator tested.

Because of this property, we can write

$$v=\frac{a_{max}}{SZ_L}, \tag{50}$$

and note particularly that v is essentially independent of V. This is important as it means that the constant of the device used as a voltmeter does not depend upon the voltage of the power supply

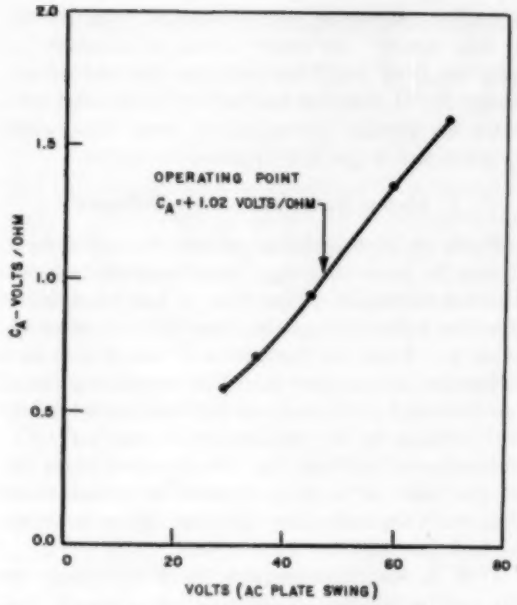

FIGURE 10.—*C_A as a function of test oscillator radio-frequency voltage at the plate.*

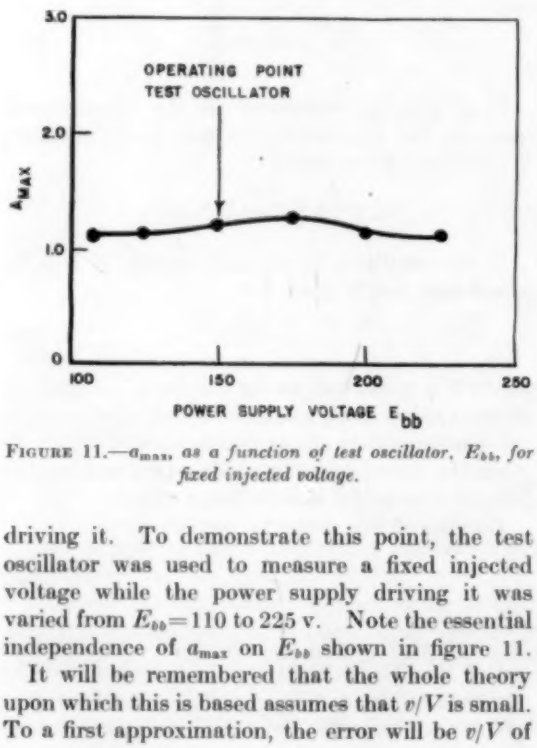

FIGURE 11.—*a_{max}, as a function of test oscillator, E_{bb}, for fixed injected voltage.*

driving it. To demonstrate this point, the test oscillator was used to measure a fixed injected voltage while the power supply driving it was varied from E_{bb}=110 to 225 v. Note the essential independence of a_{max} on E_{bb} shown in figure 11.

It will be remembered that the whole theory upon which this is based assumes that v/V is small. To a first approximation, the error will be v/V of the actual reading. Actually, figure 7 shows that the device is linear for values of a_{max} up to 2½ v.

For the measurement of large voltages a diode is sufficiently good in the frequency range in in which it is applicable. At higher frequencies, including the microwave region, the synchronized oscillator is a good device for measuring voltage as it can be calibrated with d-c instruments and known impedances. For the measurement of small voltages the linearity of the oscillator is an advantage. The lower limit at which voltage measurements can be made is set by the noise from the oscillator.

An additional advantage of the oscillator-voltmeter is its gain. It will be observed in eq 48 that there is an amplification of about five in the oscillator tested.

One large disadvantage in some applications is that the measuring oscillator couples energy into the circuit to which it is attached.

It should also be noted that the synchronized oscillator can be used, as done by Appleton, to measure small voltages by determining the band width of synchronization which is also linearly related to v by the relation

$$\Delta f = 2C_F \frac{fZ_L}{V} v. \tag{51}$$

However, C_F is relatively independent of V, and therefore V must be known accurately in order to make a measurement of v by a frequency-variation method.

If the frequency of the injected voltage cannot be varied across the synchronization band of the voltmeter, the frequency of the voltmeter can be varied across the synchronization band by a small variable condenser. The d-c grid bias or other amplitude indicator can be coupled through a blocking condenser to a peak voltmeter. As the voltmeter-oscillator is wobbled back and forth across the frequency of the injected voltage to be measured, a pulse will be observed whose peak value is a_{max}. From this pulse the size of the injected voltage can be calculated.

2. Field-Intensity Meter

The voltmeter properties of the synchronized oscillator lend themselves nicely to the measurement of field intensity at any frequency for which an oscillator is available. Appleton used the

synchronization band width of an oscillator to measure field intensities. It is proposed here to use the voltage changes directly instead of the synchronization band largely because the power-supply variation no longer enters the calculation and frequency measurements are not needed.

Assume that a small oscillator like that of figure 1 or 2 is available and that the grid bias is to be used as the indicating voltage. The first step is to determine V_g (grid-bias voltage) as a function of resistance in series with load impedance Z_L. An antenna is added across Z_L and its length adjusted so that a reasonable match is obtained. The antenna load should drop V_g to about half its unloaded value. Simultaneously the reactance of the load, Z_L, should be changed to compensate for the reactance of the antenna. This can be done by keeping the oscillator frequency constant.

From the curve of V_g as a function of r, the series-radiation resistance of the antenna R_s can be determined. (Ohmic losses in the antenna are neglected in this treatment.)

If the antenna is in a radio-frequency field of strength E (peak volts per meter), whose strength is to be measured, the field will induce a voltage, v (as already defined), in the load impedance, Z_L, of which the antenna is now a part. The magnitude of v can be shown to be

$$v=\frac{\lambda}{\pi}E\sqrt{\frac{R_sG}{120}}f(\theta), \tag{52}$$

in which G is the gain referred to an isotropic radiator, and $f(\theta)$ is the normalized radiation pattern of the antenna. If the antenna is alined with the electric field, $f(\theta)=1$. The gain, G, will be very nearly 1.5, as it will be found that quite a short dipole will load the oscillator adequately.

C_4 and S should be measured about an operating load, including the R_s of the antenna to be used. If a tuning condenser in the oscillator is wobbled back and forth through the synchronization region, a pulse of peak value a_{max} will be observed as in the case of the voltmeter. From its height the strength of the field, E, can be calculated. It will be

$$E=\frac{\pi}{\lambda}\frac{a_{max}}{SZ_L}\sqrt{\frac{120}{R_sG}} \tag{53}$$

The device can be used for the measurement of field intensities from about 10μv/m to about 1v/m. The useful range will depend on λ, but it appears that the device should work for microwaves as well as for more conventional frequencies. At microwave frequencies the antenna gain, G, can be increased to compensate for loss due to smaller λ.

As has already been mentioned, the calculation is essentially independent of the power-supply voltage. The device can be made quite simple at ordinary frequencies.

3. Linear Amplitude Modulation Detector

Inasmuch as the synchronized oscillator is a linear voltmeter it is also a linear amplitude modulation detector. Instead of reading the changes in a on a meter they can be fed directly into an audio frequency amplifier.

In this application it will be best to operate with a circuit which has $\rho=\pm\pi/2$ so that the U-W curve is a semicircle. This will be true if the signal is injected into the plate or grid circuit of a class C oscillator and the output is read from the d-c grid bias. It will be necessary to inject enough signal so that the band width of synchronization will be wide enough to include all side bands.

As the band width of synchronization is proportional to the injected voltage, the use of a synchronized oscillator poses an interesting problem. It is a linear device whose region of linear response varies instantaneously with the voltage injected. It is not immediately clear how to express the band width characteristics of such a system.

It appears reasonable to require that the time constant of the device be short compared to the shortest period of the modulation to be received. We have seen in eq 21 that an approximate time constant is

$$\tau=\frac{1}{2\pi\sqrt{\left(\frac{\Delta f}{2}\right)^2-f^2}}=\frac{1}{\pi\Delta f\sin\psi}. \tag{54}$$

Sin ψ is unity near the center of lock-in where f is nearly zero. Thus the requirement that τ be short compared to $1/f_{max}$, in which f_{max} is the highest modulation frequency to be reproduced, means that

$$\frac{1}{\pi\Delta f}<<\frac{1}{f_{max}}$$

or that

$$\pi\Delta f>>f_{max}. \tag{55}$$

Thus the signal used at the demodulator must be large enough to give a band width of about 30

kc to give faithful reproduction of 10-kc modulation.

If this turns out to be reasonable and the synchronized oscillator is used, it can give a demodulation amplification of about 5 to 10. It will also provide a measure of automatic frequency control as it will follow a deviation in carrier frequency in the intermediate frequency channel.

When nearly 100-percent modulation is used, the device will lead to distortion of a peculiar form because synchronization may be lost when the signal is small near the peak of modulation. However, the synchronized oscillator demodulator appears to present interesting possibilities worthy of further investigation.

4. Frequency Modulation Discriminator

If the oscillator circuit is arranged so that $\rho=0$ or π, the synchronized oscillator can be used as a frequency modulation discriminator demodulator. Reference to figure 1 shows that under these conditions the a curve is a straight line with $a=0$ at center frequency.

One way of achieving this is to couple an auxiliary resonant circuit to the test oscillator and inject the synchronizing signal into this auxiliary circuit. The output can be taken from the d-c grid bias of the oscillator or from a diode connected across the resonant circuit. Figure 12 shows the auxiliary resonant circuit and the coupling to the driving oscillator.

It will be assumed that the voltage is injected in series with Z_L as before. Let R represent the total resistance of the tuned circuit L, C, Z_L, and let X represent its total reactance. The resistance,

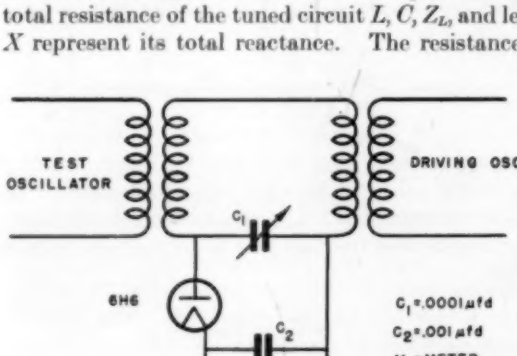

FIGURE 12.—*Auxiliary resonant circuit to obtain behavior characteristic of* $\rho=0$.

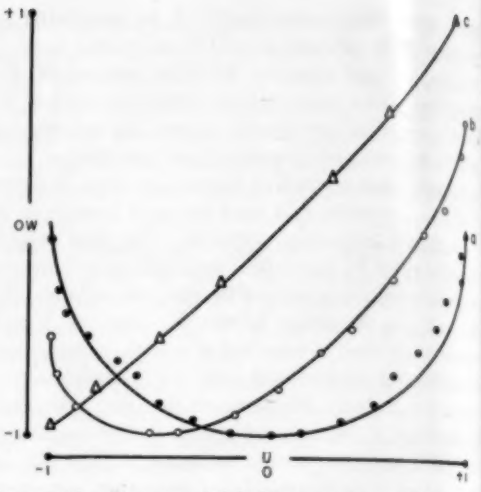

FIGURE 13.—*Experimental U-W curves for auxiliary tuned circuit.*

a, Auxiliary circuit is tuned to exact resonance; solid curve, theoretical for $\rho=0$; dots, experimental points; b, Auxiliary circuit is detuned to 90 percent of resonant voltage. c, Desired result with auxiliary circuit detuned to 70 percent of resonant voltage.

R_e, and reactance, X_e, coupled into the oscillator are then

$$R_e=\frac{(2\pi FM)^2R}{R^2+X^2}. \tag{56}$$

$$X_e=-\frac{(2\pi FM)^2X}{R^2+X^2}. \tag{57}$$

The injection of a small voltage into Z_L is equivalent to small changes in R and X in that circuit. If the circuit be detuned to the point where $R=X$ (70% of resonant voltage) small reactance changes reflect purely resistance changes, and small resistance changes reflect pure reactance changes into the oscillator.

This simple discussion neglects the changes in reactance in the auxiliary circuit due to changes in oscillator frequency. Consideration of this effect leads to important corrections but does not alter the essential argument.

If in the original oscillator $A_x=0$ and $F_r=0$, the whole system, including the tuned circuit, will behave as if $A\rho=0$ and $F_x=0$, thus making $_r=0$ or π instead of $\pm\pi/2$, which is the desired result.

Figures 13 shows a series of curves taken from the diode across the resonant circuit. Figure 13, a, shows the $U-W$ curve for exact resonance. Figure 13, b, shows an intermediate case, and

igure 13 c shows the linear relation sought at approximately 70-percent detuning.

When the arrangement described above is used as a discriminator, a will be zero at the center frequency, and the device is thus insensitive to amplitude modulation in a manner similar to a balanced discriminator.

5. Frequency modulation synchronous amplifier limiter

In this application the oscillator is locked to a frequency modulation signal. It follows the frequency variations without serious amplitude change and hence becomes a combined amplifier and limiter. It has been discussed widely in the literature.[9]

If the synchronized oscillator is capable of following frequency deviations according to the criteria established by Adler, the response to a frequency modulation signal of the form

$$f(t)=f_0 \sin 2\pi f_m t \tag{58}$$

will be a solution of

$$\frac{1}{2\pi}\frac{d\phi}{dt}+\frac{C_P v(t)}{I_0}\cos(\phi+\beta)=f(t), \tag{59}$$

in which $v(t)$ represents any amplitude modulation of v that may be present. Direct integration of eq 59 is complicated and need not be performed to the approximation needed here. It will be recalled that ϕ responds to changes in f and v with a time constant τ given by eq 21. If the changes in f or v occur in a time long compared with τ, the oscillator is essentially in equilibrium at each instant, and a succession of steady state solutions for various fixed f is a good enough approximation to the actual solution for varying f. If the injected voltage, v, is always so large that

$$Kv=nf_0;\ n>1, \tag{60}$$

then

$$\tau \leqq \frac{1}{2\pi f_0\sqrt{n^2-1}}. \tag{61}$$

As it is standard practice to have $f_0>5f_m$, it is evident that the time constant is short compared with the frequency modulation period, $1/f_m$, and the equilibrium solution, eq 20, is a reasonable approximation. Similar arguments hold for changes in v, but we are not interested in amplitude modulation here, and will henceforth assume v to be constant.

We see from eq 20 that changes in f will produce changes in ϕ so that an additional phase modulation will be added to the impressed signal. This implies $(d\phi/dt)\not\equiv 0$ in contradiction to the original assumptions made in solving eq 13 to get eq 20. The correction will be small if the frequency variations are slow, and we proceed with the approximation to write

$$\frac{d\phi}{dt}=\frac{-f}{Kv\sin(\phi+\beta)}, \tag{62}$$

and

$$F'-F=\frac{1}{2\pi}\frac{d\phi}{dt}=-\frac{f_0 f_m\cos 2\pi f_m t}{Kv\sin(\phi+\beta)}. \tag{63}$$

This makes the output-frequency deviation, f', of the oscillator have the form

$$f'=f_0\left(\sin 2\pi f_m t-\frac{f_m}{Kv\sin(\phi+\beta)}\cos 2\pi f_m t\right). \tag{64}$$

This indicates a negligible distortion when $Kv>2f_0$, as $\sin(\phi+\beta)$ is then always near unity and $f_m \ll Kv$.

Amplitude changes in v will also lead to phase modulation. However, if Kv is kept large with respect to f_0 the phase is relatively insensitive to voltage changes and the distortion arising from amplitude modulation is thereby minimized.

If the criterion $Kv=2f_0$ is set as a design center, then

$$v=\frac{2f_0}{K}=\frac{2f_0 V}{C_P Z_L}, \tag{65}$$

and the voltage amplification achieved by the use of the synchronized oscillator will be

$$\frac{V}{v}=\frac{C_P Z_L}{2f_0}. \tag{66}$$

To estimate the order of magnitude of the gain that may safely be used assume (1) that a single LC circuit is controlling the oscillator, (2) that the voltage, V, is the one across the entire inductance of the oscillating circuit, and (3) that τ is injected into this inductance. Then

$$C_P=\frac{1}{4\pi L} \tag{67}$$

[9] See, for example, C. W. Carnahan and H. P. Kalmus, Synchronized oscillators as frequency-modulation receiver limiters, Electonics **17**, 108 (1944).

and C_r is practically independent of the power-supply voltage. This gives

$$\frac{V}{v}=\frac{F}{4f_0}. \tag{68}$$

If the oscillator frequency is 10 mc and f_0 is 100 kc, the maximum voltage amplification of the device can be about 25. Of course, if the voltage across a part of the tank inductance is used as in the experiments already described, the gain is correspondingly reduced. However, gains of 15 or more should be readily obtainable. Also the voltage, v, may be injected into the grid circuit of the oscillator and the gain of the tube used to increase the voltage seen in the tank circuit. Equation 68 refers only to the voltage, v, injected into the oscillating circuit, which controls the frequency.

Unless there is some amplitude regulating device on the synchronized oscillator, there will also be an amplitude modulation in its output. The magnitude of the effect can be calculated from eq 9 and 25. It is usually small enough to be neglected.

VI. Conclusion

Although the theory and experiments just described have been discussed in terms of a conventional self-limiting source of alternating electromotive force, the concepts involved are quite general, and with appropriate redefinition of symbols, the equations can equally well apply to any source of harmonic disturbance—electrical, electromagnetic, mechanical, or acoustical, singly or in combination. The self-limitation implies that some nonlinear element is present to limit the amplitude of oscillation. A truly linear oscillator will not exhibit synchronization effe
It will, however, not appear in practice.

We may then conclude that any source of h
monic disturbance whose steady state frequen
is a function of the load applied to it, and wh
frequency can change with sufficient rapidity, w
exhibit synchronization behavior when a harmo
disturbance is impressed upon it from an exter
source. If the amplitude of the device is also
function of its load, then it will exhibit a char
teristic amplitude variation in the synchronizati
region.

We may also conclude that the source w
synchronize with an impressed disturbance, ho
ever small, if the frequency of the outside d
turbance is close enough to that of the undisturb
source.

It is important to remember that the properti
of the external source supplying the synchroniz
signal and the coupling impedance are importa
in determining the band width and phase
synchronization. If there is a considerable d
parity in the power output of the two sources, t
weaker determines the synchronization properti
of the system. If the power outputs are nea
equal, both sources contribute almost equally
its synchronization properties.

The authors are indebted to B. J. Miller a
S. Lachenbruch for many helpful contributions
the preparation of this paper, and to Robert Ad
of the Zenith Radio Corporation for an opp
tunity to study and discuss his recent paper,
Study of Locking Phenomena in Oscillators, pr
to its publication.

Washington, October 7, 1946.

S. Department of Commerce
ional Bureau of Standards

Research Paper RP1781
Volume 38, April 1947

Part of the Journal of Research of the National Bureau of Standards

Disintegration of Scandium[46]

By Irving Feister and Leon F. Curtiss

The beta and gamma radiations of scandium[46] have been studied by means of a magnetic-lens spectrometer. The beta-ray spectrum was found to be simple, with the maximum energy at 0.36 Mev. No indications were found of any other group of beta rays having energies above this value. The gamma-ray spectrum consists of two gamma rays, with energies 0.88 Mev and 1.12 Mev. These two gamma lines appear to be of equal intensity, and are therefore very probably in cascade.

I. Introduction

everal investigations have been made of the ioactivity induced in scandium by slow neu-s. The latest of these reported in the litera-by Walke [1][1] states that there are two groups isintegration electrons, the main group having aximum energy of 0.26 Mev, and the other up, less than 5 percent as abundant as the n group, having a maximum energy of 1.5 v. Walke also reports a single gamma ray of gy 1.25 Mev. These values of beta- and ma-ray energies were obtained by means of orption measurements in Al and in Pb, respec-ly.

ecently a table of radioactive isotopes was ed by the Manhattan District [2]. According his table, the maximum energy of the beta from Sc^{46} is 0.4 Mev, and the gamma-ray trum consists of only one gamma ray of gy 1.4 Mev. The table does not indicate how e values were obtained.

he beta- and gamma-ray energies for Sc^{46} rted in the present paper were obtained by ns of a spectrometer of the thin magnetic-lens developed by Deutsch, Elliott, and Evans This instrument is described by Miller and tiss [4]. The results obtained are completely ariance with those reported by Walke. The maximum energy of the beta rays agrees fairly well with that given in the Manhattan District table [2], but the number and energies of the gamma rays do not agree with the data in that table.

II. Preparation of Sources

Sc^{46} was prepared for the present experiments by the reaction Sc^{45} (n, γ). A sample of scandium oxide was irradiated with slow neutrons for over 2 months in the Clinton pile. The half-life of Sc^{46} has been accurately determined by Walke [1] as 85 ± 1 days.

The beta-ray source for the spectrometer is shown in figure 1, B. A thin Al foil mounted on a Lucite holder provided the backing for the source. The foil was moistened with a very thin layer of dilute glyptal solution, on which a small amount of the radioactive scandium oxide powder was deposited. The holder was designed to reduce back-scattering to a minimum.

Figure 1, A, shows the gamma-ray source used in the spectrometer. The active sample was placed in a small brass container whose walls were thick enough to absorb all the beta radiation emitted. A uranium radiator was used because both the photoelectric yield and the difference between the *K*- and *L*-electron binding energies are greatest in uranium, thus giving the most intense *K*- and *L*-photolines and the greatest separation between these lines (see fig. 4).

ures in brackets indicate the literature references at the end of this

734742—47——2

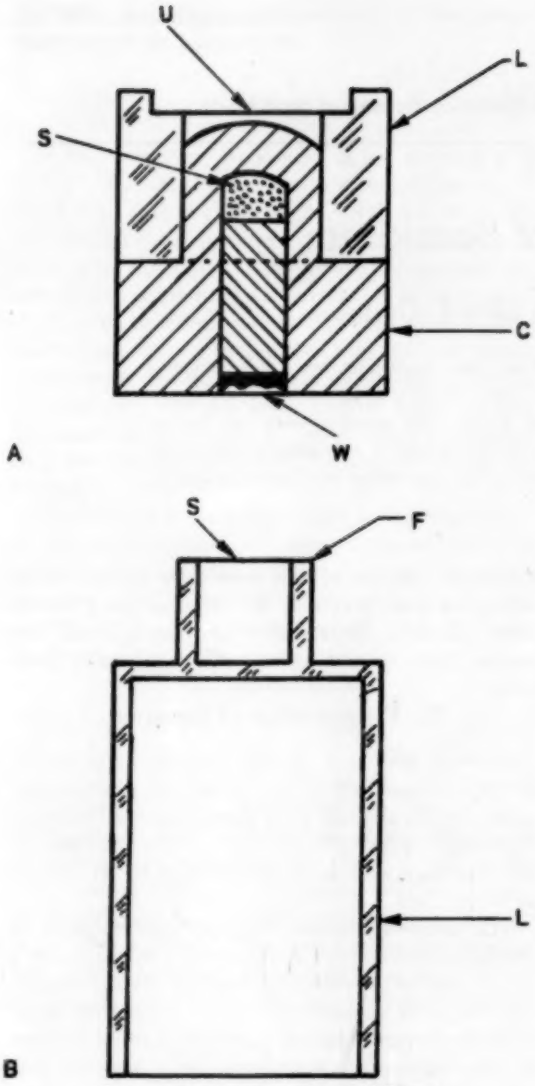

FIGURE 1.—*Section of source holders.*

A, For producing secondary photoelectrons from a uranium radiator by Sc^{46} gamma rays: *U*, thin uranium foil; *L*, Lucite collar; *S*, radioactive Sc^{46}; *C*, brass capsule; *W*, wax seal. *B*, For introducing Sc^{46} into the spectrometer for measurement of primary beta rays: *S*, thin deposit of Sc^{46} on aluminum foil, *F*; *L*, Lucite support.

III. Beta-Ray Spectrum of Sc^{46}

The beta-ray spectrum of Sc^{46} is shown in figure 2. The quantity N is equal to $P/H\rho$, where P is the number of pulses per minute in the Geiger-Müller counter; N represents the relative intensity over equal intervals of $H\rho$ [3, 5]. The symmetry of the beta-ray distribution indicates that the beta-ray spectrum is simple and consists of only a single group of electrons, which is confirmed by the Fermi plot (fig. 3). This is contrary to the results reported by Walke [1], who indicated the presence of two groups of electrons, the second being less than 5 percent as abundant as the main group. The absence of low-energy electrons with $H\rho < 670$ is due to absorption in the source and mica window (2.8 mg/cm²) of the counter.

The Fermi plot for Sc^{46} is shown in figure 3. The departure from linearity of the Fermi plot in the low-energy range is very probably due to the distortion of the beta-ray spectrum at low energies because of scattering in the source and absorption in the mica window of the counter. The maximum energy of the beta rays, as obtained from figure 3, is 0.358 ± 0.008 Mev. This is in

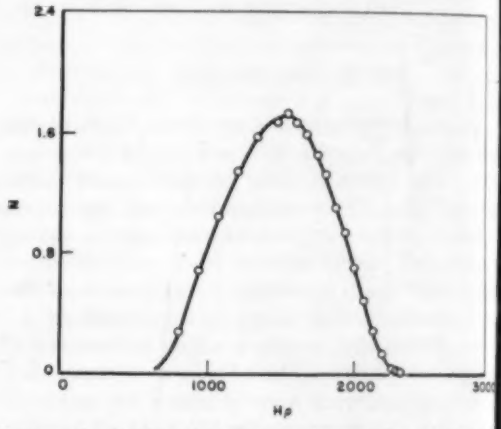

FIGURE 2.—*Primary beta-ray spectrum of Sc^{46} showing intensity plotted against $H\rho$.*

Sc^{46} (85 days); beta-ray spectrum.

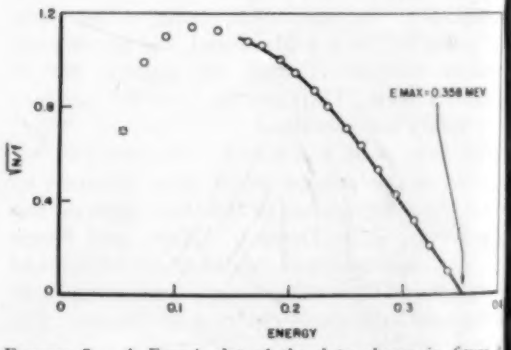

FIGURE 3.—*A Fermi plot of the data shown in figure 2.*

Sc^{46} (85 days); Fermi plot.

irly good agreement with the value 0.4 Mev ported by the Manhattan Project [2]. No indi- tion was found of any other group of dis- tegration electrons having a maximum energy 1.5 Mev, as reported by Walke [1].

IV. Gamma Rays of Sc^{46}

The energies and approximate relative in- nsities of the gamma rays from Sc^{46} are deduced om the photoelectric conversion spectrum shown figure 4. Here, again, N is equal to $P/H\rho$. he curve shows the spectrum of secondary ectrons ejected from a uranium radiator (and om the brass capsule containing the source) by e gamma rays of Sc^{45}. The continuous dis- ibution is due to Compton recoil electrons, ostly from the brass capsule, whereas the peaks e due to K- and L-electrons expelled from the -radiator by the gamma rays from Sc^{46}. Figure shows the presence of two gamma rays. Their ergies may be determined from the K-photo- nversion lines by adding the K-binding energy uranium (0.118 Mev) to the K-electron energies served. We thus obtain 0.883 ± 0.01 and 116 ± 0.02 Mev, respectively, for the two gamma- y energies. As a further check on these results, e same gamma energies are also determined m the less intense L-photoconversion lines in gure 4, using the L-binding energy of uranium

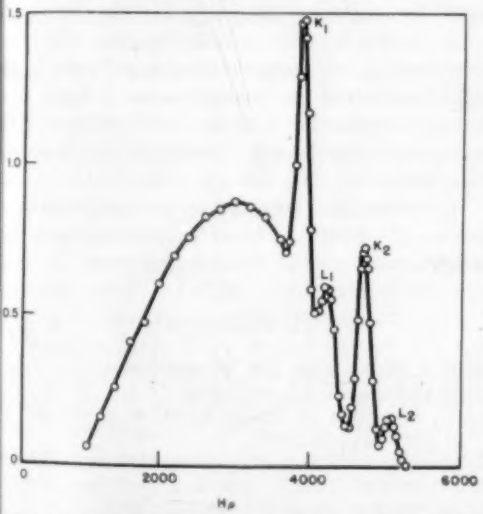

GURE 4.—*Seconondary electron spectrum produced by Sc^{46} gamma rays in uranium.*

K_1, L_1 are conversion lines of a 0.883-Mev gamma ray. K_2, L_2 are from a 1.116-Mev gamma ray. Sc^{46} (85 days); gamma rays; uranium radiator.

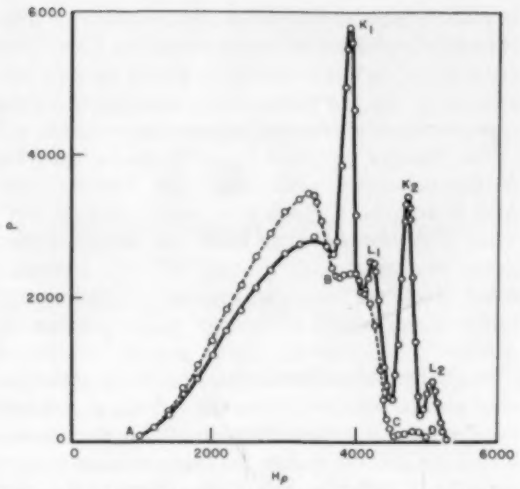

FIGURE 5.—*Comparison of secondary electron distributions produced by Sc^{46} gamma rays with and without uranium radiator.*

Sc^{46} (85 days); gamma rays;——gamma spectrum, uranium radiator; ..... without uranium radiator.

(0.022 Mev). The values thus obtained, 0.882 and 1.117 Mev, agree very closely with those given above.

These results are completely at variance with those of Walke [1], who reports only a single gamma ray from Sc^{46} with 1.25-Mev energy. They also disagree with the table recently published by the Manhattan District [2], according to which Sc^{45} emits only one gamma ray with 1.4-Mev energy.

The relation between the continuous Compton distribution and the photoelectric conversion spectrum of figure 4 is clearly shown in figure 5. Here P, the number of pulses per minute in the Geiger-Müller counter, is plotted against $H\rho$ instead of N. The full curve is the distribution obtained with the U-radiator in place (see fig. 1, A). The broken curve is the distribution obtained from the same source without the U-radiator. The broken curve has three distinct parts: A to B is due to Compton electrons expelled from the brass capsule by both gamma rays of Sc^{46}; B to C is due to Compton electrons expelled by the 1.12-Mev gamma ray alone; and C to D is very probably due to photoelectrons ejected from the brass capsule by the 1.12-Mev gamma ray.

It is seen from figure 5 that the number of Compton electrons obtained without the U-radiator

in place is greater than with the U-radiator. This is readily explained by the fact that the U-radiator (42 mg/cm²) is thick enough to stop a considerable number of the Compton electrons from the brass capsule, especially in the lower energy region.

The broken curve in figure 5 shows that the K_1-photoelectron peak lies just beyond part A to B and the K_2 peak just beyond part B to C. This is in accord with what we would expect, since the maximum energy of the Compton recoil electrons from gamma rays in this energy range is only about 80 percent of the gamma-ray energy.

Siegbahn [5] has shown that the gamma energies may also be obtained from the inflection points of the Compton distribution curve. This was likewise done here, and the values thus obtained are in good agreement with the values as determined above. This latter method, however, is less accurate than the above, so that it is of use here primarily as an approximate check on the gamma energies obtained from the photolines.

V. Disintegration Scheme of Sc^{46}

A rough estimate of the relative intensities of the two gamma rays may be obtained from the relative heights of the K_1 and K_2 photoelectron peaks in figure 4. As a first approximation, the photoelectric absorption coefficient may be said to vary according to a law intermediate between E^{-2} and E^{-3}, where E is the gamma-ray energy, probably nearer E^{-2} for gamma rays in this energy range [6]. If we take the photoelectric absorption coefficient to be approximately proportional to E^{-2} and assume that the gamma rays are of *equal intensity*, then the ratio of the photoelectron intensities expelled from the uranium radiator by the two gamma rays of Sc^{46} is

$$\frac{I_{k1}}{I_{k2}} \cong \frac{1.12^2}{0.88^2} \cong 1.6.$$

Figure 4 shows that the ratio of the heights of the K_1 and K_2 peaks is about 1.5. The effect of finite radiator thickness (42 mg/cm²) on the heights of the K_1 and K_2 photoelectron peaks is to reduce the height of the K_1 peak more than that of the K_2 peak, since the latter consists of more energetic electrons less likely to be absorbed in the radiator. Therefore, the observed relative heights of the K_1 and K_2 peaks in figure 4 are seen to be in approximate agreement with the ratio of equation (1), which is based on the assumption that the two gamma rays are of equal intensity.

The above considerations do not, of course, definitely prove that the two gamma rays emitted by Sc^{46} are of equal intensity, but they do suggest strongly that such is actually the case. It seems very likely that the two gamma rays are in cascade, and that the disintegration scheme is as shown in figure 6. The order of emission of the two gamma rays is not determined by the present experiment.

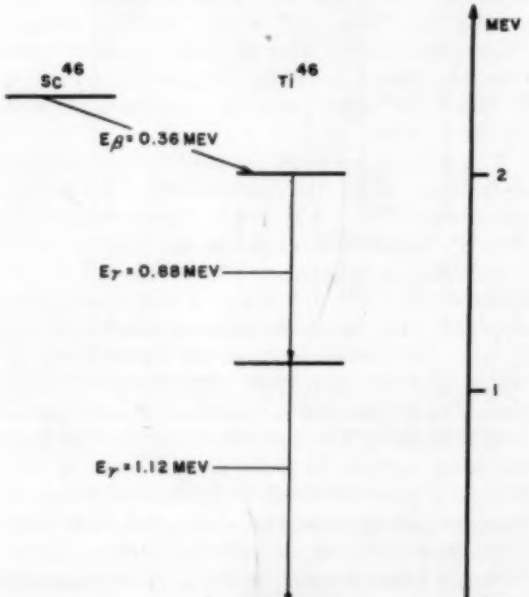

FIGURE 6.—*Suggested disintegration scheme for Sc^{46} based on the measured beta- and gamma-ray spectra.*

In conclusion, we express our appreciation to Leonard C. Miller,[2] who set up and calibrated the spectrometer used in these experiments.

VI. References

[1] H. J. Walke, Phys. Rev. **57,** 163 (1940).
[2] Rev. Sci. Instr. **17,** 348 (1946).
[3] M. Deutsch, L. G. Elliott, and R. D. Evans, Rev. Sci. Instr. **15,** 178 (1944).
[4] L. C. Miller and L. F. Curtiss, J. Research NBS (1947) RP1778.
[5] K. Siegbahn, Phys. Rev. **70,** 127 (1946).
[6] L. H. Gray, Proc. Camb. Phil. Soc. **27,** 103 (1931).

WASHINGTON, February 13, 1947.

[2] Now at Clinton Laboratories, Oak Ridge, Tenn.

U. S. Department of Commerce
National Bureau of Standards

Research Paper RP1782
Volume 38, April 1947

Part of the Journal of Research of the National Bureau of Standards

High-Temperature X-Ray Diffraction Apparatus

By Alvin Van Valkenburg, Jr., and Howard F. McMurdie

A furnace for obtaining X-ray powder diffraction patterns of samples at elevated temperatures has been designed and constructed. This furnace is used with the Norelco X-ray spectrometer, in which the photographic film is replaced by a Geiger counter. The assembly has the following advantages over previously described high-temperature X-ray powder diffraction cameras: (1) Any number of patterns can be obtained without intermediate cooling of the sample, (2) in 40 minutes the pattern is produced in a form ready for study, and (3) patterns can be obtained at temperatures up to 1,500° C. The diffraction data for the α form of $2CaO.SiO_2$ are given.

I. Introduction

Many crystalline substances exhibit structure changes on heating, different modifications being stable at different temperatures. The method most commonly used to investigate modifications that are unstable at room temperatures is to hold a specimen at a temperature above an inversion and quench. In many cases, the form stable at the higher temperature is thereby preserved for examination at room temperature and can be studied by X-ray diffraction or optical methods. Unfortunately, some substances revert on quenching to the original form. Therefore, a determination at high temperature must be made while the specimen is held at an elevated temperature.

For this reason, and also to study in greater detail the processes of inversion, it is desirable to have equipment by which X-ray diffraction patterns can be made at elevated temperatures.

Various cameras have been designed for such work [1, 2, 3, 4][1], but in general they have been confined to temperatures below 800° C. For work in ceramics, and particularly in refractories, it is often desirable to study changes that take place at temperatures appreciably higher. Patterns obtained at elevated temperatures were reported in Germany [5], but details of the furnace are lacking. One factor that has prevented the use of higher temperatures is the problem of cooling the photographic film. H. Friedman's development [6] of an X-ray powder diffraction apparatus using a Geiger counter in place of a film and its commercial production have helped solve this problem.[2] This apparatus covers the arc from 45 to 5 degrees of Bragg angle in 40 minutes, the pattern being recorded on a strip chart with 1 inch equal to 1 degree. Either Cu or Fe radiation can be used.

In the present paper, a furnace for use with the Geiger-counter X-ray spectrometer is described. With this equipment, X-ray powder diffraction patterns can be made on samples at temperatures up to 1,500° C.

II. Construction of furnace

The furnace, cylindrical in shape and heated electrically, is mounted midway between the X-ray tube and the Geiger counter (figs. 1 and 2). The brass base (G, fig. 3) is inserted in place of the specimen holder supplied regularly with the X-ray spectrometer. This base (or platform) has a central recessed area for an Alundum disk and pedestal (F, fig. 3) that supports the 80-percent-platinum–20-percent-rhodium specimen holder (E,

[1] Figures in brackets indicate the literature references at the end of this paper.

[2] This equipment is made available commercially by the North American Philips Co.

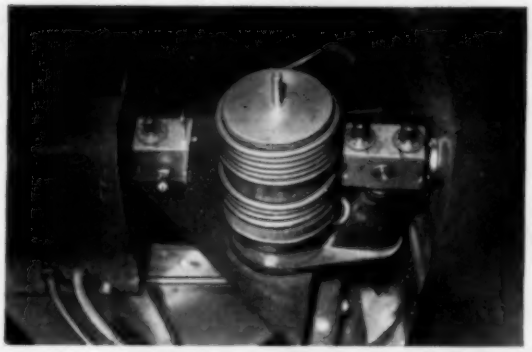

FIGURE 1.—*Over-all view of furnace in place in X-ray spectrometer.*

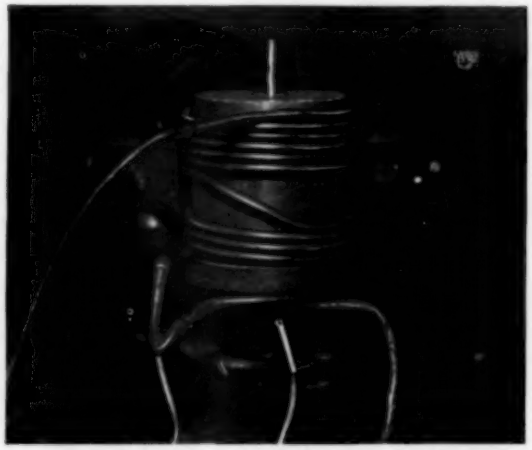

FIGURE 2.—*Furnace in place.*

figs. 3, and 4). This specimen holder has a groove in the base, which fits a ridge on the ceramic pedestal, thereby assuring correct alinement of the holder. Surrounding the ceramic pedestal and specimen holder are a two-unit heating element (*D*, fig. 3) and two shields (*B* and *C*, fig. 3) which are alined by grooves in the ceramic base (fig. 5), and a third shield (A, fig. 3) which is alined by a groove in base, *G*.

The heating element consists of an 80-percent-platinum–20-percent-rhodium wire winding on two coaxial Alundum tubes, which have windows cut in them at the specimen level for transmission of the X-ray beam. These tubes are shown separated in figure 6. The wire is placed in grooves on the outside of each tube. The inner tube at the window level has an additional opening cut in the rear and, in the front, that part of the tube between the windows has the winding placed o both sides. The outer tube at the window lev has the winding doubled back on the rear sectio of tube. These windings at the window leve combined with the opening cut into the rear the inner tube, give direct radiation to the fro and rear of the platinum specimen holder. Th two sets of windings are connected in series. Th heating element is shown in place on the base figure 7.

The innermost of the three shields (*C*, figs. and 8) is a radiating shield of 80-percent platinum 20-percent-rhodium; the intermediate shield (*B* figs. 1 and 8) is made of stainless steel; the thi shield (*A*, figs. 1 and 8) forms the outer shell a is made of brass. Each shield contains tw openings for X-ray transmission at the specime level. The windows of the outer shell are cover with thin sheets of beryllium (*I*, fig. 3) to preve heat radiation to adjacent parts and to minimi air currents within the furnace. Water-cooli

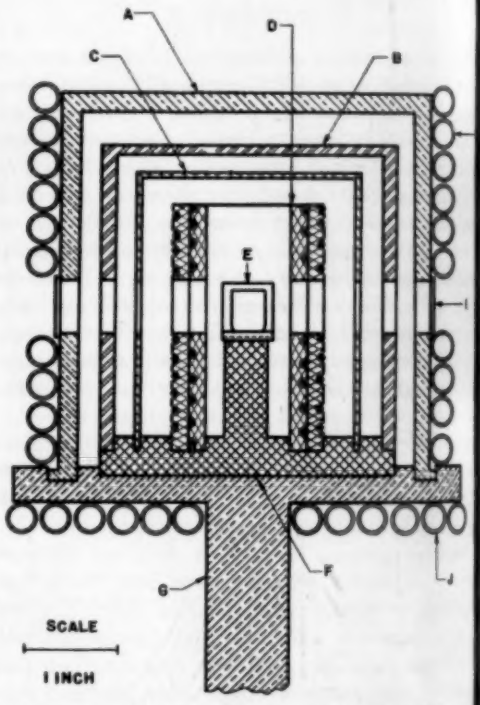

FIGURE 3.—*Cross section of X-ray diffraction furnace.*

A, Brass outer shell; *B*, intermediate steel shield; *C*, platinum radia shield; *D*, heating unit with platinum windings; *E*, specimen holder Pt-20% Rh); *F*, ceramic base; *G*, brass base; *H*, water-cooling co beryllium cover to window; *J*, water-cooling coil.

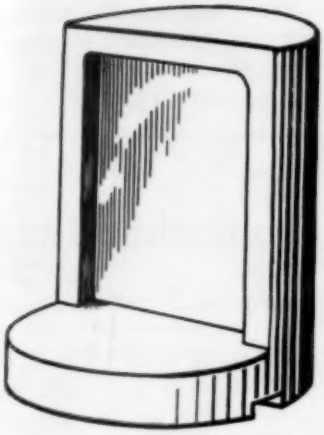

FIGURE 4.—*Specimen holder.*

80 percent Pt-20 percent Rh.

FIGURE 5.—*Ceramic base and specimen holder.*

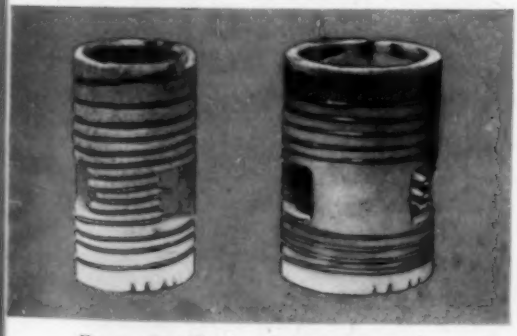

FIGURE 6.—*Heating elements separated.*

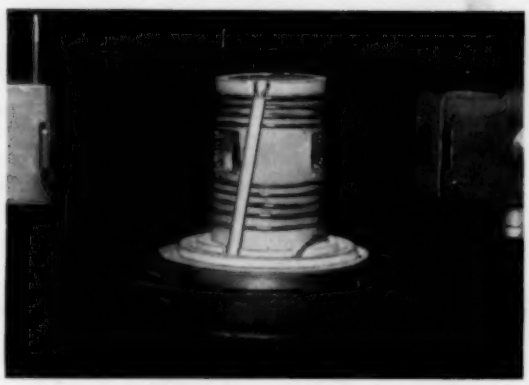

FIGURE 7.—*Heating element on ceramic base, showing thermocouple leads.*

FIGURE 8.—*Shields.*

A, Outer brass case with cooling coil; *B*, intermediate steel shield; *C*, platinum radiation shield.

coils placed beneath the brass base and around the outer shell are indicated by *J* and *H* in figure 3 and shown in figure 2.

The furnace is heated with 110-v alternating-current controlled by two variable autotransformers so that the secondary of the first feeds the primary of the second. At 1,500° C the furnace requires about 12 amp at 60 v. The furnace is maintained automatically within ±1 deg C.

The temperature of the furnace is measured and controlled by a platinum–10-percent-rhodium thermocouple connected to an electronic-recording potentiometer. The wires are enclosed in a ceramic tube placed vertically alongside the heating element (fig. 7). At the top of the heating element, the bare thermocouple wires are bent over the edge, and the junction is directly in front of the specimen holder.

The following simple procedures are necessary to prepare the furnace for operation: (a) Removing the three shields, *A*, *B*, and *C;* (b) setting the

specimen holder, *E*, with the powdered sample pressed into the recessed face, upon the pedestal, and (c) replacing the shields. Parts *G*, *F*, and *D* do not need to be disturbed.

An X-ray spectrometer equipped with a furnace like the one described has the advantage that the pattern is available for inspection at once without the necessity of photographic processing. Also, a second pattern at a different temperature can be made immediately without cooling the sample to room temperature.

III. High-Temperature Form of $2CaO.SiO_2$

Thermal studies have shown that a change takes place at about 1,420° C in $2CaO.SiO_2$ [7]. However, material quenched from above 1,500° C does not give an X-ray pattern different from β-$2CaOSiO_2$. Bredig [8], by analogy with K_2PO_4, postulated that α-$2CaO.SiO_2$ must be hexagonal with an axial ratio of about 1.29. Greene [9] was able to quench an impure $2CaO.SiO_2$ (with Al_2O_3 and Na_2O present) and obtain a sample that gave an X-ray pattern indicating a hexagonal cell with $A=5.44$ kX and $C=7.02$ kX.

With the equipment described in this paper, a pattern of pure $2CaO.SiO_2$ was obtained at 1,500° C. The data given in table 1 agree with the data from the impure sample used by Greene. This shows that α-$2CaO.SiO_2$ is hexagonal, isostructural with K_2PO_4 and with $A=5.08$ kX and $C=7.05$ kX.

TABLE 1.—*Diffraction data for* $2CaO.SiO_2$ *at 1,500° C*

hkl	*d/n*	Relative intensity
	kX	*Percent*
102	2.84	85
110	2.69	100
201	2.25	30
202	1.970	55
122	1.603	15
300	1.576	15
114	1.501	8
220	1.368	3
132	1.280	2

The authors thank L. G. Cossette for his help in preparing the ceramic base and for his help and suggestions on winding the heating coil.

IV. References

[1] A. H. Jay, Z. Krist. **86,** 106 (1933).
[2] L. Backhurst, Proc. Roy. Soc. (London) [A] **102,** 340 (1923).
[3] A. Westman and G. Pragmen, Z. physik. Chem. [B] **102,** 1 (1922).
[4] M. J. Buerger, N. W. Buerger, and F. G. Chesley, Am. Mineral. **28,** 288 (1943).
[5] Otto Raff and Fritz Ebert, Z. anorg. allgem. Chem. **180,** 19 (1929).
[6] H. Friedman, Electronics **18,** 132 (1945).
[7] A. A. Rankin and F. E. Wright, Am. J. Sci. [4] **39,** 1 (1915).
[8] M. A. Bredig, J. Phys. Chem. **46,** 747 (1942).
[9] K. T. Greene, J. Research NBS **32,** 1 (1944) RP1570.

WASHINGTON, January 23, 1947.

U. S. Department of Commerce
National Bureau of Standards

Research Paper RP1783
Volume 38, April 1947

Part of the Journal of Research of the National Bureau of Standards

Heats of Combustion and Isomerization of Six Nonanes

By Walter H. Johnson, Edward J. Prosen, and Frederick D. Rossini

The heats of isomerization of six of the nonanes were determined by measurement of the ratios of the heats of combustion in the liquid state of purified samples of these compounds by the procedure previously described for other hydrocarbons. The data yield the following values for the heat of isomerization in the liquid state at 25° C, $\Delta H°$, of *n*-nonane into the other nonanes, in kilocalories per mole: *n*-Nonane, 0.00; 3,3-diethylpentane, −0.01 ±0.33; 2,2,3,3-tetramethylpentane, −0.70 ±0.31; 2,2,3,4-tetramethylpentane, −0.56 ±0.22; 2,2,4,4-tetramethylpentane, −1.11 ±0.25; 2,3,3,4-tetramethylpentane, −0.62 ±0.35. These data were combined with the value previously reported for the heat of combustion of *n*-nonane to obtain values for the heats of combustion of the other five nonanes in the liquid state at 25° C.

I. Introduction

In continuation of the program of determining the heats of combustion, formation, and isomerization of hydrocarbons of various types [1, 2, 3, 4, 5, 6, 7] [1] calorimetric measurements have been made that yield values for the differences in the heats of combustion, or the heats of isomerization, of six of the isomeric nonanes in the liquid state at 25° C. These heats of isomerization were combined with the value [8] previously reported for the heat of combustion of *n*-nonane to obtain values for the heats of combustion of the other five nonanes in the liquid state at 25° C.

II. Unit of Energy, Molecular Weights, Uncertainties

The unit of energy upon which the values reported in this paper are based is the international joule, derived from mean solar seconds and the units of international ohms and international volts, in terms of which certification of standards of resistance and electromotive force is made by the Bureau. For conversion to the conventional thermochemical calorie, the following relation is used [9]:

1 calorie = 4.1833 international joules.

The molecular weight of carbon dioxide, the mass of which was used to determine the amount of reaction, was taken as 44.010, from the 1941 table of international atomic weights [10].

The uncertainties assigned to the various quantities dealt with in this paper were derived, where possible, by a method previously described [11].

Definitions of the symbols used are given in previous papers [1, 3, 4, 6, 7].

III. Method and Apparatus

The same method and apparatus were used as in the investigations recently reported from this laboratory [1, 2, 3, 4, 5, 6, 7, 12]. One calorimeter system was used throughout this investigation. Resistance bridge No. 404 and platinum resistance thermometer No. 373,730 were used for all the experiments reported here.

No products of incomplete combustion were found in any of the experiments.

IV. Materials

The compounds used in the present investigation were samples from the API–NBS series of highly purified hydrocarbons, which are being prepared through a cooperative undertaking of

[1] Figures in brackets indicate the literature references at the end of this paper.

the American Petroleum Institute and the National Bureau of Standards [15, 16, 17].

These samples of API–NBS hydrocarbons have been made available by the AmericanPetroleum Institute and the National Bureau of Standards through the API Research Project 44 on the "Collection, Analysis, Calculation, and Compilation of Data on the Properties of Hydrocarbons." The samples were purified at the National Bureau of Standards by the API Research Project 6 on the "Analysis, Purification, and Properties of Hydrocarbons", from material supplied by the following laboratories:

3,3-Diethylpentane and 2,2,3,3-tetramethylpentane, by the American Petroleum Institute Research Project 45 at the Ohio State University, Columbus, Ohio, under the supervision of C. E. Boord.

2,2,3,4-Tetramethylpentane, 2,2,4,4-tetramethylpentane, and 2,3,3,4-tetramethylpentane, by the National Advisory Committee for Aeronautics, through its Aircraft Engine Research Laboratory, Cleveland, Ohio, and its supported work in the Automotive Section at the National Bureau of Standards.

n-Nonane, by the American Petroleum Institute Research Project 6 at the National Bureau of Standards.

A complete description of the purification, purity, and freezing points of the six nonanes of the present investigation is given by Streiff, Murphy, Cahill, Flanagan, Sedlak, Willingham, and Rossini [17], who reported the amounts of impurity in these samples, as determined from measurements of freezing points, to be as follows: *n*-Nonane, 0.0006 ±0.0004; 3,3-diethylpentane, 0.00013 ±0.00011; 2,2,3,3-tetramethylpentane, 0.0006 ±0.0002; 2,2,3,4-tetramethylpentrane, 0.00024 ±0.00014; 2,2,4,4-tetramethylpentane, 0.0011 ±0.0008; 2,3,3,4-tetramethylpentane, 0.00044 ±0.00037, mole fraction.

As the manner of purification of these compounds [17] was such as to leave substantially only close-boiling isomeric impurities in the respective compounds, it is calculated that in the worst case the measured heat of combustion would be affected by less than 0.001 percent because of impurities in the compound.

V. Results

The experimental results of the present investigation are summarized in table 1, which gives for each of the six compounds the following data: The number of experiments performed; the minimum and maximum values of the mass of carbon dioxide formed in the combustion and of the calorimetric quantities k, K, U, ΔR_c, Δr_i, Δr [1]; the mean value of B, and its standard deviation, in ohms per gram of carbon dioxide formed as defined by equation 4 of reference [1]. The symbols have the same significance as in the previous report [1], and the references there cited.

In table 2 are given, for the six nonanes, values of the following: The constant B in ohms per gram of carbon dioxide, as given in table 1; $B°$, which is B corrected to the ideal bomb reaction by the

TABLE 1.—*Results of the calorimetric combustion experiments*

Compound (liquid)	Number of experiments	Mass of carbon dioxide formed	k	K	U	ΔR_c	Δr_i	Δr_n	B	
									Mean	Standard deviation of mean
		g	*min*$^{-1}$	*Ohm*	*Ohm*	*Ohm*	*Ohm*	*Ohm*	*Ohm*/*g*CO_2	*Ohm*/*g*CO_2
n-Nonane	5	2.53916 to 2.61484	0.001979 to .001990	0.001023 to .001326	0.000227 to .000242	0.287491 to .299007	0.000415 to .000430	0.000043 to .000056	0.1130485	±0.000092
3,3-Diethylpentane	6	2.53532 to 2.65980	0.001974 to .001984	0.000866 to .001271	0.000160 to .000309	0.287080 to .301067	0.000415 to .000426	0.000050 to .000054	.1130482	±.000086
2,2,3,3-Tetramethylpentane	6	2.45440 to 2.56627	0.001971 to .001997	0.001154 to .001518	0.000094 to .000328	0.277761 to .290464	0.000411 to .000427	0.000050 to .000054	.1129942	±.000050
2,2,3,4-Tetramethylpentane	5	2.52718 to 2.63979	0.001974 to .001984	0.00891 to .001317	0.000187 to .000291	0.289006 to .298752	0.000416 to .000430	0.000050 to .000056	.1130049	±.000029
2,2,4,4-Tetramethylpentane	7	2.51035 to 2.67953	0.001976 to .001995	0.000777 to .001477	0.000162 to .000294	0.283988 to .303077	0.000415 to .000431	0.000036 to .000044	.1129624	±.000061
2,3,3,4-Tetramethylpentane	5	2.53247 to 2.86449	0.001977 to .001991	0.000558 to .001427	0.000269 to .000374	0.286688 to .324037	0.000234 to .000424	0.000040 to .000046	.1130014	±.000095

TABLE 2.—*Heats of isomerization and combustion in the liquid state*

Compound	B, at 28.00° C	B°, at 28.00° C	Ratio of the heats of combustion in the ideal bomb process, B_i°/B_n°, at 28.00° C	Difference in the heats of combustion in the ideal bomb process $(-\Delta U^\circ)_n-(-\Delta U^\circ)_i$, at 28.00° C
	Ohm/gCO₂	*Ohm/gCO₂*		*Int. kj/mole*
n-Nonane	0.1130485 ±0.0000164	0.1130214 ±0.0000164	1.000000	0.00
3,3-Diethylpentane	.1130482 ±0.0000196	.1130211 ±0.0000198	0.999997 ±0.000227	0.02 ±1.39
2,2,3,3-Tetramethylpentane	.1129942 ±0.0000180	.1129674 ±0.0000180	.999522 ±0.000215	2.92 ±1.31
2,2,3,4-Tetramethylpentane	.1130049 ±0.0000052	.1129779 ±0.0000050	.999615 ±0.000152	2.35 ±0.93
2,2,4,4-Tetramethylpentane	.1129624 ±0.0000102	.1129354 ±0.0000102	.999239 ±0.000171	4.65 ±1.04
2,3,3,4-Tetramethylpentane	.1130014 ±0.0000210	.1129734 ±0.0000214	.999575 ±0.000238	2.60 ±1.45

Compound	Heat of isomerization of the liquid, $H_i^\circ(\text{liq})-H_n^\circ(\text{liq})$, at 25.00° C		Heat of combustion of the liquid, $-\Delta H_c^\circ$, at 25.00° C	
	Int. kj/mole	*kcal/mole*	*Int. kj/mole*	*kcal/mole*
n-Nonane	0.00	0.00	6123.51 ±0.75	1463.80 ±0.18
3,3-Diethylpentane	−0.02 ±1.39	−0.01 ±0.33	6123.49 ±1.58	1463.79 ±0.38
2,2,3,3-Tetramethylpentane	−2.92 ±1.31	−0.70 ±0.31	6120.59 ±1.51	1463.10 ±0.36
2,2,3,4-Tetramethylpentane	−2.35 ±0.93	−0.56 ±0.22	6121.16 ±1.19	1463.24 ±0.28
2,2,4,4-Tetramethylpentane	−4.65 ±1.04	−1.11 ±0.25	6118.86 ±1.28	1462.69 ±0.31
2,3,3,4-Tetramethylpentane	−2.60± 1.45	−0.62 ±0.35	6120.91 ±1.63	1463.18 ±0.39

method of Washburn [13];[2] B_i°/B_n°, which is equal to the ratio of the heat evolved, per mole of hydrocarbon, in the ideal bomb process at 28° C for each isomer to that of *n*-nonane; $(-\Delta U^\circ)_n-(-\Delta U^\circ)_i$, the difference, between *n*-nonane and each isomer, in the heat of combustion in the ideal bomb process at 28° C; H_i° (liquid)$-H_n^\circ$ (liquid), the heat of isomerization of *n*-nonane into each isomer, at 25° C and 1 atmosphere, for the liquid state; and $-\Delta H_c^\circ$, the decrement in the heat content accompanying the reaction of combustion of the hydrocarbon in the liquid state in oxygen to form gaseous carbon dioxide and liquid water, with all the reactants and products in their thermodynamic standard states at 25° C.

The value of the heat of isomerization was obtained by means of the relation [1]:

$$(-\Delta U^\circ)_n-(-\Delta U^\circ)_i=(-\Delta U^\circ)_n(1-B_i^\circ/B_n^\circ).$$

For this calculation, the value of $(-\Delta U^\circ)_n$ at 28° C was taken as 6110.2 int. kj/mole [3]. The value of the heat of combustion of a given isomer was obtained by appropriately combining the heat of isomerization with the heat of combustion of *n*-nonane as given by the equations [8]

$$C_9H_{20}\ (n\text{-nonane, liquid})+O_2(\text{gas})=9CO_2(\text{gas})+10H_2O(\text{liquid})$$

$$\Delta H^\circ_{298.16}=-6123.51\ \pm0.75\ \text{int. kj/mole}=-1463.80\ \pm0.18\ \text{int. kcal/mole}.$$

All the uncertainties assigned to the experimental quantities in table 2 (except the heats of combustion) are equal to twice the standard deviation of the mean. The uncertainties assigned to the values of the heats of combustion were obtained by combining [11] the uncertainty in the value of the heat of combustion of *n*-nonane [8] with the uncertainties in the values of the heats of isomerization. The uncertainty to be assigned to the value of the heat of isomerization of any one of the isomers into any other one may conservatively be taken as ±0.30 kcal/mole.

The experimental data of the present and previous investigations on the paraffin hydrocarbons are being correlated to yield heats of combustion

[2] The Washburn correction is the same for all these compounds as they are isomers, but account is taken of the variation of the correction with the amount of sample burned. As used here, the Washburn correction was modified to apply to 28° C and to the gases at zero pressure (instead of 1 atmosphere).

and formation of the remaining 29 nonanes which have not been subjected to experimental measurement, with general formulas for calculating values for the decanes and higher paraffin hydrocarbons [14].

VI. References

[1] E. J. Prosen and F. D. Rossini, J. Research NBS **27,** 289 (1941) RP1420.

[2] E. J. Prosen and F. D. Rossini, J. Research NBS **27,** 519 (1941) RP1439.

[3] E. J. Prosen and F. D. Rossini, J. Research NBS **33,** 255 (1944) RP 1607.

[4] E. J. Prosen, R. Gilmont, and F. D. Rossini, J. Research NBS **34**, 65 (1945) RP1639.

[5] E. J. Prosen and F. D. Rossini, J. Research NBS **34,** 163 (1945) RP1635.

[6] W. H. Johnson, E. J. Prosen, and F. D. Rossini, J. Research NBS **35,** 141 (1945) RP1665.

[7] W. H. Johnson, E. J. Prosen, and F. D. Rossini, J. Research NBS **36,** 463 (1946) RP1715.

[8] E. J. Prosen and F. D. Rossini, J. Research NBS **34,** 263 (1945) RP1642.

[9] E. F. Mueller and F. D. Rossini, Am. J. Phys. **12,** 1 (1944).

[10] G. P. Baxter, M. Guichard, O. Hönigschmid, and R. Whytlaw-Gray, J. Am. Chem. Soc. **63,** 845 (1941).

[11] F. D. Rossini and W. E. Deming, J. Wash. Acad. Sci. **29,** 416 (1939).

[12] E. J. Prosen and F. D. Rossini, J. Research NBS **33,** 439 (1944) RP1619.

[13] E. W. Washburn, BS J. Research **10,** 525 (1933) RP546.

[14] E. J. Prosen and F. D. Rossini, National Bureau of Standards. Unpublished data.

[15] A. R. Glasgow, Jr., E. T. Murphy, C. B. Willingham, and F. D. Rossini, J. Research NBS **37,** 141 (1946) RP1734.

[15] A. J. Streiff, E. T. Murphy, V. A. Sedlak, C. B. Willingham, and F. D. Rossini, J. Research NBS **37,** 331 (1946) RP1752.

[17] A. J. Streiff, E. T. Murphy, J. C. Cahill, H. F. Flanagan, V. A. Sedlak, C. B. Willingham, and F. D. Rossini, J. Research NBS **38,** 53, (1947) RP1760.

WASHINGTON, November 6, 1946.

U. S. Department of Commerce
National Bureau of Standards

Research Paper RP1784
Volume 38, April 1947

Part of the Journal of Research of the National Bureau of Standards

Structure of Difructose Anhydride II

By Emma J. McDonald and Anne L. Turcotte

The structure of difructose anhydride II is shown to be 2,1′-4,2′-difructofuranose. 3,4,6-Trimethylfructose has been identified as one of the hydrolysis products of hexamethyl difructose anhydride II. This has been accomplished by a chromatographic separation with subsequent identification of 3,4,6-trimethylglucosazone.

I. Introduction

The difructose anhydrides include four well-defined crystalline sugars. Diheterolevulosan was first prepared by Pictet and Chavan [1][1] by the action of concentrated hydrochloric acid on fructose at 0° C. This sugar is a difructopyranose in which carbon atoms 1 and 2 of each fructose residue are joined to form a dioxane ring. The other members [2,3] of this group are designated difructose anhydrides I, II, and III, all of which are found in the reaction product when inulin is hydrolyzed with acid. Difructose anhydride I has been shown [4] to be a difructofuranose in which the two fructose residues are joined as they are in diheterolevulosan. Difructose anhydride III [5] has been identified as difructofuranose in which carbon atoms 1 and 2 of one fructose residue unite with carbons 2 and 3 of the other, again forming a dioxane ring. Previous work, as will be briefly reviewed, has indicated the structure of difructose anhydride II which we now show conclusively to be 2,1′-4,2′-difructofuranose.

McDonald and Jackson [5] hydrolyzed the hexamethyl derivative of difructose anhydride II and found that the specific rotation of the hydrolysis product in aqueous solution was approximately +25 degrees. This positive rotation indicated the presence of fructofuranose rather than pyranose derivatives. In the latter case one would expect a negative rotation. Upon treatment with phenylhydrazine, an oil resulted that could not be identified.

In a later investigation McDonald and Jackson [6] studied the reaction of the difructose anhydrides with periodic acid. In keeping with their known structures, difructose anhydrides I and III and diheterolevulosan consumed, respectively, 2, 1, and 4 moles of acid per molecule of sugar. One mole of periodic acid reacted with each molecule of difructose anhydride II.

In order to verify the position of the rings in the fructose residues of this sugar, the following procedure has been carried out: Hexamethyl difructose anhydride II was hydrolyzed in hydrochloric acid solution and the resulting trimethylfructose mixture converted to the corresponding methylfructosides. Further methylation, followed by removal of the glycosidic methyl groups, gave a tetramethyl fructose having a specific rotation in aqueous solution of +31.0 degrees. This agrees with that reported for tetramethylfructofuranose ($[\alpha]_D^{20}=+31.3°$, in water) and excludes the pyranose derivative ($[\alpha]_D^{20}=-121.3°$, in water). By establishing the ring structure of the fructose residues, the only assumption made by McDonald and Jackson when they proposed the following for-

[1] Figures in brackets indicate the literature references at the end of this paper.

mulas as the possible structures for difructose anhydride II has been removed:

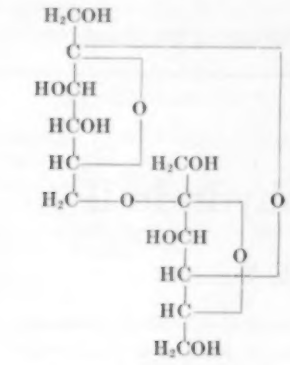

(1)

2,4′-6,2′-Difructofuranose

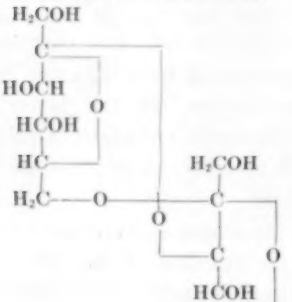

(2)

2,3′-6,2′-Difructofuranose

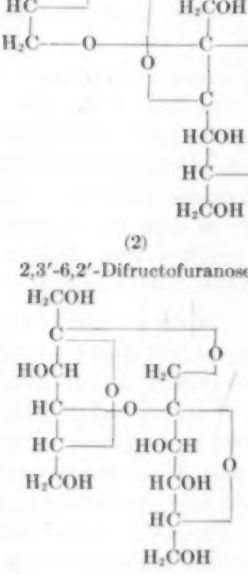

(3)

2,1′-4,2′-Difructofuranose

The sugar whose structure is shown by (3) upon hydrolysis would yield 3,4,6- and 1,3,6-trimethylfructose. Formulas (1) and (2) represent sugars whose hexamethyl derivatives on acid treatment would be converted to 1,3,4-trimethylfructose along with 1,3,6- or 1,4,6-trimethylfructose. Since the sugar of formula (3) is the only one in which methylation and hydrolysis would yield 3,4,6-trimethylfructose, identification of this substance as one of the hydrolysis products of the hexamethyl derivative would exclude all other possibilities and establish the structure of difructose anhydride II as 2,1′-4,2′-difructofuranose.

As previously stated, McDonald and Jackson obtained an oil when the hydrolysis product of the hexamethyl derivative was reacted with phenylhydrazine. By a chromatographic process crystalline 3,4,6-trimethylglucosazone has been separated and identified as one of the constituents of this reaction product. The structure of difructose anhydride II is therefore established as 2,1′-4,2′-difructofuranose (formula 3).

II. Experimental Procedure

1. Purification of 3,4,6-Trimethylglucosazone

3,4,6-Trimethylfructose and its phenylosazone were prepared from inulin according to the method of Haworth and Learner [7]. The osazone, which

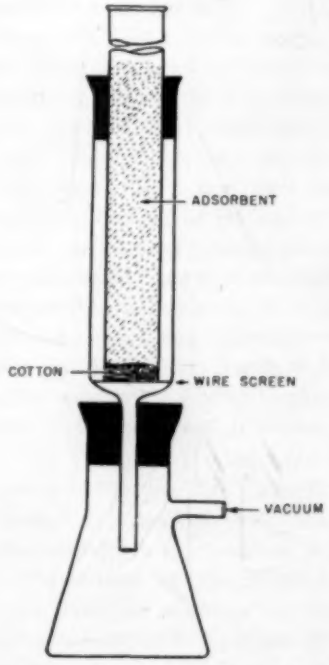

FIGURE 1.—*Apparatus for chromatographic adsorption.*

separated as a dark-red oil from the reaction mixture, was washed with water and air-dried. Instead of following the procedure for crystallization, this viscous material was dissolved in carbon tetrachloride and purified by adsorption on a chromatographic column.

The adsorption column was prepared from Magnesol,[2] using Celite as a filter aid in the proportion of 5 parts (by weight) of Magnesol to 1 part of Celite. A column about 17 cm in length was formed by packing 7 g of the mixture in a glass tube 11 mm in diameter, using suction. (See fig. 1.) Best results were obtained when the column was wet with pure solvent previous to the addition of the solution containing not more than 50 mg of osazone. About 500 ml of carbon tetrachloride was necessary to properly develop this chromatogram.

The column consisted of four distinct bands, the largest of which was the bright yellow area containing the glucosazone. This yellow band, about 8 cm in length, was preceded by a brown zone approximately one-fourth this length. An orange ring appeared immediately below the glucosazone and the lower portion of the column took on a pink color as the chromatogram was developed. It was noted that exposure to sunlight caused a surface discoloration, indicating decomposition. Hence in subsequent separations a paper covering was used to protect the column from light.

The yellow portion of the column was removed and the osazone extracted with alcohol. After evaporation the residue crystallized from an aqueous alcohol solution. The osazone was filtered and recrystallized several times from an ether-petroleum ether mixture, mp 138° C (uncorrected).

2. 3,4,6-Trimethylglucosazone from Difructose Anhydride II

Five grams of hexamethyl difructose anhydride II was hydrolyzed at 95° C for 160 minutes in 0.8 *N* hydrochloric acid solution. The yellowish solution was neutralized with barium carbonate and evaporated to dryness in vacuum. The methylfructoses were extracted with chloroform and the solvent evaporated.

[2] A synthetic hydrated magnesium acid silicate ($2MgO.5SiO_2$).

The mixture of trimethylfructoses (0.5 g) was digested with 10 ml of dilute acetic acid and 0.75 g of phenylhydrazine at 100° C for 20 minutes, at which time a large amount of a dark-red oil had separated. This oil was washed with water, and 50-mg portions, dissolved in carbon tetrachloride, were purified by means of an adsorption column containing Magnesol, as previously described.

The chromatogram contained the same large yellow area preceded by a brown zone and followed by an orange ring. There was an additional narrow red band at the top of the column, and at the bottom of the column a yellow zone formed, which was slowly eluted.

The portion containing the osazone was removed and extracted with alcohol. After evaporation of the solvent, the residue was taken up in carbon tetrachloride and added to another Magnesol column. A bright-yellow zone with a small amount of dark material at the top of the column resulted after approximately 300 ml of carbon tetrachloride was passed through. The yellow band was extracted with ether and evaporated to a concentrated solution. Petroleum ether was added to a faint turbidity and in a short time crystals appeared. After repeated recrystallization from ether-petroleum ether, a melting point of 136° C (uncorrected) was obtained, which remained constant after further recrystallization. A mixture of this material and 3,4,6-trimethylglucosazone melted at 137° C (uncorrected).

III. References

[1] A. Pictet and J. Chavan, Helv. Chim. Acta **9,** 807 (1926).

[2] R. F. Jackson and S. M. Goergen, BS J. Research **3,** 27 (1929) RP79.

[3] R. F. Jackson and E. J. McDonald, BS J. Research **6,** 709 (1931) RP299.

[4] W. N. Haworth and H. R. L. Streight, Helv. Chim. Acta **15,** 693 (1932).

[5] E. J. McDonald and R. F. Jackson, J. Research NBS **24,** 181 (1940) RP1277.

[6] E. J. McDonald and R. F. Jackson, J. Research NBS **35,** 497 (1945) RP1683.

[7] W. N. Haworth and A. Learner, J. Chem. Soc. **1928,** 619.

WASHINGTON, December 9, 1946.

U. S. Department of Commerce
National Bureau of Standards

Research Paper RP1785
Volume 38, April 1947

Part of the Journal of Research of the National Bureau of Standards

Mangabeira Latex and Rubber[1]

By Norman Bekkedahl and Waldemar Saffioti[2]

The tree *Hancornia speciosa*, more commonly known as the mangabeira, which grows in several of the tropical states of Brazil, yields a rubber-containing latex. This tree is very well known for the delicious fruit (mangaba) it bears, but it does not have such a good reputation for the quality of rubber it produces. The natives of Brazil coagulate this rubber by means of solutions of alum or sodium chloride. It has been found, however, from this investigation that if these coagulating agents are replaced by dilute hydrochloric acid or by the latex from another tree, the caxinguba (*Ficus anthelmintica*), a rubber of much improved properties can be produced.

I. Introduction

The mangabeira (*Hancornia speciosa*) is a small tree, or large shrub, of the Apocynaceae family. It is indigenous to the eastern and southern states of Brazil and also to parts of the Amazon Valley. It is cultivated mostly for its fruit (mangaba), which is edible and has an excellent taste. When an incision is made into the bark of this tree, however, it yields a rubber-containing latex. Its rubber is known usually as mangabeira rubber or Pernambuco rubber.

Before World War II there was very little commercial production of mangabeira rubber, although it had been marketed to some extent before plantation rubber became prominent and when the price of crude rubber was very high. Several factors accounted for this low production. The most commonly used natural rubber, which is obtained from the seringueira, or Pará, rubber-tree (*Hevea brasiliensis*),[3] is superior both in quality and as a general-purpose rubber. The more effective tapping methods for the manabeira are much different from those for the seringueira and have not yet been as well developed. The methods for coagulating rubber from the latex of mangabeira are somewhat different from those of the seringueira and are not generally as well known to the natives or producers.

During the war, however, efforts were made to obtain all the natural rubber possible, almost regardless of cost or quality. According to information made available by E. G. Holt [1],[4] who had charge of all statistical records of the Rubber Development Corporation, mangabeira rubber was produced during the war years to the total extent of about 2,000 to 2,500 tons. The use, and consequently the production, of this rubber will probably decrease again to a negligible quantity when normal conditions are resumed unless improved processes are developed for tapping the mangabeira tree and for coagulating the rubber from the latex, or unless special uses are found or developed that require the softness or other properties peculiar to this rubber.

A thorough study of tapping methods could undoubtedly bring about a greater yield of latex per tree per year with less effort on the part of the producer. The present methods of tapping in-

[1] The experimental work for this paper was performed during 1943 and 1944 at the Instituto Agronômico do Norte, at Belém do Pará, Brazil, where the senior author was detailed for the purpose of establishing a rubber laboratory for the Brazilian Government. This article is also to be published as a technical bulletin of the Instituto Agronômico do Norte, entitled "Latex e Borracha de Mangabeira", I. A. N. Boletim Técnico No. 11.

[2] Present address: Alameda Glette 463, São Paulo, Brazil.

[3] *Hevea brasiliensis* is the botanical name for the Pará rubber tree, named after the port of Pará at the mouth of the Amazon River through which all the rubber passed in the early days of wild-rubber production. In Brazil this tree is more commonly known as the seringueira, and this term is often used in this paper. It must not be confused with *seringueiro*, which is the term applied to the person who taps the seringueira and processes its latex into rubber.

[4] Figures in brackets indicate the literature references at the end of this paper.

734742—47——3

volve either the cutting of many V-notches in the bark of the tree, not only on the main trunk but also on all the larger branches, or the cutting of spiral grooves in the main trunk, which are fed from straight cuts on the branches. The latex flows very freely from these wounds into cups placed just below the V's or at the bottom of the spiral, and within an hour or two a liter or more of latex may be obtained from a single tree. This process is quite different from the tapping of the seringueira, or Pará, rubber-tree, which is usually tapped by making only one straight slanting cut at a time on the trunk of the tree within a few feet of the ground. Each tapping of the Pará tree may yield an average of only about 50 to 100 ml of latex, but this cutting is repeated usually every second day throughout most of the year. The mangabeira tree, like the castilloa, does not produce such a copious quantity of latex at each tapping if the process is repeated at these frequent intervals. A. W. J. Dyck [2] has observed that in Bahia the mangabeira trees are tapped generally no more than two to three times per year. The maximum quantity of rubber that a mangabeira tree can produce during a full year of tapping is not known, but under proper conditions it may possibly yield as much as, if not more than, the Hevea. At least, the amount of labor connected with the tapping of a mangabeira tree over a period of a year would be considerably less than that with the Hevea.

The coagulating characteristics of mangabeira latex are much different from those of the seringueira latex. All the mangabeira latices studied by the present authors were found to be very stable with regard to spontaneous coagulation. No coagulations took place from long-time standing under the atmospheric conditions of the tropics. No putrefaction took place from bacterial action. No coagulation occurred by the addition of acetic or formic acid in concentrations used on the plantations for the coagulation of Hevea latex, which is equivalent to about 1 g or less of the concentrated acid per liter of the latex. However, if 100 times this quantity of glacial acetic acid is added to undiluted mangabeira latex, the rubber will coagulate. The addition of this large quantity of acid is, of course, not economical or practical on a commercial basis.

Because of possible variations that may occur in the same species of tree in different localities, there may be some variations in the minimum quantities of coagulants required for quantitative coagulation. All the latices studied in this investigation, which were obtained from areas adjoining the lower Amazon, were found to be very stable. Several samples of mangabeira latex obtained in the Amazon Valley remained stable and fresh after more than a year of standing without the addition of a preservative. Dyck [2], who studied methods of coagulating mangabeira latex he obtained from the state of Bahia, on the east coast of Brazil, reports that mangabeira latex is much more stable than Hevea latex. Guimaraes and Chaves [3], who worked with mangabeira latex from southern Brazil, state that no coagulation took place either by fermentation or by the addition of enzymes. It is doubtful, then, whether there is sufficient variability in latices from different areas that would appreciably alter the conclusions arrived at from a study of coagulants from the commercial viewpoint.

The natives of Brazil, who coagulate rubber from Pará latex by means of smoking the latex on the end of a stick or paddle, have found that this procedure is not as satisfactory a method for the latex of the mangabeira. They have, however, discovered that ordinary table salt or alum solutions in moderate quantities will separate the rubber from mangabeira latex, and therefore they use these coagulants in their processing operations.

Mangabeira rubber seems to have gained a bad reputation with the consumer, especially as to its aging qualities. It was therefore thought worthwhile to make a search for other coagulants and to study the rubber produced under various processing conditions. At the same time it was decided to make a few simple analyses and tests on the latex and the rubber of the mangabeira.

II. Samples of Latex

All the latex samples used in these experiments were obtained from mangabeira trees found in various parts of the lower Amazon Valley. On most occasions representatives were sent out from the rubber laboratory to these areas to purchase the latex. The producers, in all instances, claimed there had been no dilution of their latices, either through intention or by rainfall. However, in order to be sure of authentic

material, latex that had undergone no adulteration or dilution, for at least some of the experiments, the authors on several occasions procured their own samples, conducting all the operations themselves, such as tapping the trees, collecting the latex, and transporting it to the laboratory. They collected their samples on the Island of Marajó. The most concentrated sample came from some mangabeira trees near the city of Ponte de Pedras on this same island. In each case about 5 gallons of the latex was obtained for experimentation.

III. Experimental Procedure

Immediately after reaching the laboratory the latex samples were strained through fine Monel-metal sieves in order to remove dirt, bark, and other solid foreign matter that may have been present. Before portions of the samples were removed for experimentation, the latex was stirred well in order to be sure of a homogeneous mixture.

1. Method for Measuring Density

All density measurements on the latex samples were made by means of a glass hydrometer that had a range from 0.940 to 1.000. The markings on the scale were 0.001 unit, and it was fairly easy to estimate the next place to within 2 or 3 units. The hydrometer had previously been calibrated by measuring the densities of alcohol-water mixtures, the true densities of which had been determined by weighing known volumes. All density measurements reported in this paper are corrected to or measured at the temperatures indicated, and the units are given in grams per milliliter (g/ml).

For several samples of latex, density measurements were made at various temperatures in order to obtain a value for the thermal coefficient of expansion. For these experiments a portion of the sample was placed in a 2-liter cylinder and then cooled for about 24 hours in a refrigerator to about 8° C. Then, with constant and rapid agitation (by means of a motor-stirrer) between hydrometer readings, density-temperature data were taken. The warming of the solution was either natural or by an electric immersion heater controlled by a variable-ratio autotransformer. The usual temperature rise was 10° C per hour or slower.

2. Methods for Determining Rubber Content of Latex

Analyses were made on several samples of the mangabeira latex for both the total solids (TS) and the dry rubber content (DRC).

In determining the TS content, a sample of the latex was weighed before and after drying on the surface of a glass or glazed porcelain plate. It was found most convenient to use plates thin enough for low weight and small enough to fit on the pan of an analytical balance. The latex sample was weighed from a covered weighing flask because evaporation of even a small portion of the latex affects the accuracy of the analytical results. The plates were weighed before the latex was added and after the drying of the latex. The latex should not form too thick a layer on the plate for proper evaporation. Preliminary drying of the latex may take place in the room, either free or by forced circulation of air, but final drying must take place in an oven. A temperature of about 70° C is quite suitable for the drying. In the present investigation, the weight of the samples ranged from 0.5 to 25 g. For the smaller samples much more care is required, and it is recommended that larger samples be used. Samples of about 10 g each can be handled conveniently and give excellent results.

For the determination of the DRC of the latex several coagulants were tried in varying proportions. Weighed samples of the latex, usually about 100 g each, were placed in crystallizing dishes and the coagulating agents added with stirring. In some cases the latex had been diluted with water previous to the addition of the coagulant. After coagulation was complete, which could easily be determined by the clarity of the serum, and the coagulum was strong enough to handle, it was passed several times between laundry-type wringer rolls for sheeting, during which process plenty of water was used for washing, and then it was hung up to air-dry for several hours. The rubber was then passed through a laboratory-size mixing mill for creping. The resulting creped rubber was placed in an oven at 70° C until dry. In order to make sure that the samples were dry, they were usually folded and

passed through the mill again to give a fresh surface before the second oven-drying.

A large number of coagulants were originally tried, but only a few of these showed any promise of being satisfactory. Therefore, most of the study of coagulating agents was limited to a few, namely, acetic acid, alum solution, sodium chloride solution, hydrochloric acid, and latex of the caxinguba tree (*Ficus anthelmintica*).

3. Methods for Coagulating Latex

In addition to the methods of coagulation mentioned in the previous section, which were made for the purpose of analyses only, studies were also made on methods which might be applicable on a commercial scale. For this purpose the coagulations were performed in either galvanized-iron or wooden containers of about 24 by 35 cm dimension and 12 cm in height.

One liter of the undiluted latex was used for each experiment. Sometimes the latices were diluted with water previous to the addition of the coagulants. Stirring took place during the addition of the coagulating agent. After the coagulum had been allowed to stand a sufficient time in order for it to develop strength enough to be handled, it was passed several times between wringer rolls for the purpose of pressing into a thinner sheet. Between the pressing operations the rubber was washed thoroughly. It was next passed between ribbed rolls from which the rubber emerged in the usual form of plantation ribbed smoked sheet. It was then either hung up in a ventilated drying room at 40° C, or placed in a smoke hut at the same temperature until dry. These drying operations usually required from 4 to 7 days.

4. Methods of Chemical Analysis

Only a few different chemical analyses were made on the mangabeira rubber. It was not necessary to determine the moisture content because all the samples were previously dried. Ash determinations were made by igniting the samples carefully in a muffle furnace according to the directions given in section 17, of method D297–41T of the ASTM [4]. The resin content of the rubber was assumed to be the same as the acetone-extract determined by the procedure in section 11 also given in method D297–41T.

5. Methods of Vulcanization and Testing

Samples of the mangabeira rubber, usually 250 to 300 g each, were compounded on a 6 by 12-in. laboratory-size mixing mill according to Formula II of the Crude-Rubber Committee of the Rubber Division of the American Chemical Society [5]:

Rubber	100 parts.
Zinc oxide	6.0 parts.
Sulfur	3.5 parts.
Stearic acid	4.0 parts.
Mercaptobenzothiazole	0.5 part.

The compounded rubber was vulcanized at 141° C in standard molds of the type described in method D15–41 of the ASTM [4]. Samples were vulcanized for various periods of time, ranging from 15 minutes to several hours, in order to include the optimum conditions of vulcanization for each sample of rubber as determined by the highest tensile strength. In all cases the time for vulcanization of the mangabeira rubber at 141° C to the optimum conditions was either 60 or 90 minutes, more frequently the latter. This rubber therefore cures slightly slower than the Pará rubber. The vulcanized rubber sheets were cut into dumbbell-shaped specimens, and the tensile properties were measured by means of a Scott tensile tester. All tensile values are reported in kilograms per square centimeter (kg/cm^2) of original cross section of the specimen. When aging experiments were performed, some of the dumbbell specimens were aged in a pressure bomb for 48 hours at 70° C and under 300 $lb/in.^2$ (21.1 kg/cm^2) of oxygen pressure. The rubber specimens were then tested for tensile strengths and the results compared with those of the unaged specimens.

IV. Results and Discussion

1. Total Solids and Rubber in Latex

The true values of the DRC of several of the latices, which are determined by the method of complete coagulation, are given in column 7 of table 1. Column 8 contains the corresponding values for the TS, as determined by the method of evaporation.

Eight different samples of latices are designated A through H. The sample 0.5H is latex H diluted 1:1 with water. Sample 37 is a theoretical latex having a density of 0.9748 g/ml at 30°C. Its purpose will be seen later, but it can have no

TABLE 1.—*Densities, coefficients of expansion, and rubber content of several mangabeira latices*

Sample or substance	Densities, g/ml at—			Coefficient, $\frac{1}{V}\left(\frac{dV}{dT}\right)$	DRC		TS by evaporation method
	20° C	25 °C	30° C		Densities	Coagulation	
					Wt %	*Wt %*	*Wt %*
A	0.9877	0.9861	0.9844	34×10^{-5}	28.8	25.5	.....
B	.9856	.9838	.9819	38	30.9	27.4	30.1
C	.9868	.9848	.9827	42	30.3	30.4	.....
D	.9875	.9856	.9836	40	29.5	32.1	36.1
E	.9828	.9810	.9791	38	33.3	33.1	35.5
F	.9815	.9794	.9771	45	35.0	34.0	36.8
G	.9827	.9806	.9783	45	34.0	37.3	.....
H	.9777	.9755	.9730	48	38.5	39.7	43.0
0.5H	.9876	.9864	.9851	25	28.2	19.8	21.5
37	.9787	.9768	.9748	40	37.0	.....	.....
Water	.9882	.9971	.9957	25	19.5	0	0
Serum	.....	.....	1.0200	.....	0	0	.....
Disperse phase	.....	.....	0.9064	.....	100	100	100
Rubber	.9142	.9110	.9077	65	98.7	100	100

experimentally determined DRC and TS. The water, as shown in the table, of course, runs zero in DRC and TS. The serum of any latex is also zero in DRC. The serum probably would have a TS content of about 2 to 3 percent, but this determination was not made experimentally. The disperse phase is assumed to be all rubber, and therefore is 100 percent in both DRC and TS.

As with latex from the Pará tree, the TS of mangabeira latex is 5 to 10 percent greater than the DRC. The serum contains some nonrubber constituents that are not separated from it by the addition of the coagulating agents in the determination of the DRC.

2. Density and its relation to rubber content

Because of the noncommercial value of mangabeira rubber in the past there has been very little scientific information published about this rubber. The present authors were unable to find in the literature any data on the physical constants or properties of the rubber or latex. It has been found from experiments performed in this investigation, however, that the DRC and density values for mangabeira latex are very similar to those for the Pará latex. Therefore, for comparisons, a brief survey of a few of the more prominent published investigations made on the Hevea latices will be included in the discussion.

For many years the plantations of the Far East, for control purposes in the field and in the processing factories, have been using density measurements of their Hevea latices as a means of determining their DRC. As latex is composed of rubber particles suspended in a serum (and not in true solution) the law of mixtures has been assumed—the volume percentage of rubber in the latex is a linear function of the density.

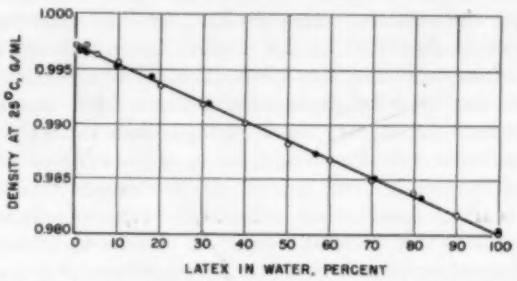

FIGURE 1.—*Density values of a sample of mangabeira latex at different dilutions with water.*

The two types of points indicate separate experiments on the same batch of latex.

In order to test the validity of this law of mixtures for latex, an experiment was performed in which density measurements were made on a sample of mangabeira latex for a series of dilutions. The results are plotted in figure 1. It can be seen that the concentration of the rubber, or DRC, is a linear function of the density, the latter value, after continued dilution, approaching that for water (0.9971 g/ml at 25°C). This curve could therefore be used to determine the amount of dilution of this particular sample of latex, but it could not be used to determine the DRC of other samples of latex because the rubber particles are not suspended in water but in a serum whose density is not the same as that for water.

Various authors have made contributions to the study of density values versus DRC. The results disagree with each other to some extent, but this disagreement is probably within the variations found between different samples of latex. Very few of the authors have defined their units of density or specific gravity, nor have they recorded the temperatures at which these determinations were made. DeVries [6] states that the specific gravity of the serum of Hevea latex varies between 1.016 and 1.025 for different latices, but for calculations he uses a value of 1.020. He accepts a specific gravity of 0.914 for the rubber phase in the latex. The curve on page 4 of his book [6] is made linear between these two values on a weight-

percentage basis, whereas it should have been on a volume-percentage basis in order to comply with the law of mixtures.

It seems to have been common practice on plantations, because of the high viscosity of undiluted latex, to dilute the latex 1:1 with water before measuring the density, and then to multiply the resulting value of DRC by 2 in order to obtain the DRC of the original latex. DeVries points out that this procedure gives erroneous results because continuous dilution with water causes the density curve to approach the value of water, as is shown in figure 1, and not the value of the serum. Of course, the accuracy of these results in most instances need not be great because latex is not generally sold on this basis. This type of analysis is made on the plantation in order to determine quickly whether or not the coolies are diluting the latex before bringing it in, and also in order to determine the approximate extent of dilution of the latex in preparation for coagulation.

Hauser [7] states that for the calculations of DRC in the average latex a value of 0.914 may be assumed for the specific gravity of the disperse phase, thus giving it a DRC value of 91.4 g/100 ml. Hauser's curve gives the rubber content in grams per 100 ml on a linear basis between this point and one at 1.020 specific gravity for the pure serum. Scholz and Klotz [8] found a lower value of 0.901 for the disperse phase.

Rhodes [9], who experimented with about 850 different samples of latex and probably made more precise measurements under better controlled conditions than the other investigators, extrapolated an experimentally obtained linear curve of specific gravity versus rubber content to values below 28 percent and above 50 percent of rubber on the weight basis. From this he obtained a density of 1.0177 for the pure serum and 0.9019 for that of the rubber phase. DeVries [10] made some calculations by using part of the data obtained by Rhodes, and replotted the DRC on a volume basis instead of a weight basis. From these he obtained 1.020 and 0.9065 as the specific gravities of the serum and the disperse phase, respectively. Rhodes [11] later agreed with the latter method of calculation, and recomputed all of his previous data, arriving at the values of 1.0200 and 0.9064 for the extreme points on the curve. Stevens and Stevens [12] prepared a table comparing the values obtained by the Rubber Research Institute of Malaya (Rhodes' values) and their own values at the Rubber Trade Association and found them to be in very close agreement.

By repeated electrophoretic depositions of rubber from latex, and redispersing the rubber in ammoniacal solutions, Schmidt and Stamberger [13] prepared a rubber dispersion free from its original serum. On progressive dilutions of this final dispersion density values were determined, and an extrapolation of the curve gave a density of 0.905 for the disperse phase at 18° C. After drying the disperse phase, its density was measured by a direct determination as 0.909 at the same temperature. Using 0.000658/deg C as the volume-temperature coefficient of expansion for rubber [14], these densities are calculated to be equivalent to 0.901 and 0.905, respectively, at 25° C. These do not agree very well with the density value of 0.911 g/ml obtained by Curtis, McPherson, and Scott [15], which has been suggested by Wood [16] as the best value determined for rubber. The previously mentioned values of 0.905 and 0.909 at 18° C also are equivalent to 0.898 and 0.902, respectively, for 30° C, which is the temperature probably close to the average at which the measurements of density are made on plantations.

The density of 0.911 g/ml for rubber at 25° C, which was previously referred to as the probable best value, is equivalent to 0.908 g/ml at 30° C. This value is in quite close agreement with the value of 0.9064 obtained by Rhodes, who reported that all his measurements were made at 29° to 30° C. As Rhodes' value comes closest to that obtained by the direct measurement of density of rubber, and as he seems to have done very careful work on many samples of latex of variable composition, his results should be the most acceptable at present. There appears to be no doubt as to the density of the average serum being 1.020. From the equation given by Rhodes, the following can be derived:

$$\text{DRC}=\frac{0.9245-0.9064D}{0.1136D},$$

in which D is the density of the latex in grams per milliliter at 30° C.

Although all of the authors admit quite a large variation or deviation in the individual results, probably because of interfacial tensions producing

a frictional effect, Hauser [7] claims this frictional effect can be eliminated by the addition of a small quantity of sodium hydroxide or potassium hydroxide, thus resulting in a much better value for the DRC. However, no hydroxide was added to any of the latices studied in this investigation.

In figure 2 are plotted the values of densities of several samples of mangabeira latex at temperatures ranging from about 10° to 45° C. It was not possible in most cases to make measurements above 35° C because some rubber coagulated on the blades of the stirring propeller. This separation of the rubber from the latex, of course, changes the DRC and therefore the density of the latex.

From the curves in figure 2 the density values of the several samples of latex can easily be read at various temperatures. Values of the densities at 20°, 25°, and 30° C for the various samples of latex have been determined from a large-scale drawing of these curves and are recorded in columns 2, 3, and 4, respectively, of table 1. Densities are reported at 25° C because this temperature has become the most common for reporting values of physical constants. The 30° C values are reported because they come closer to being those representing measurements made in the tropical climates of the rubber plantations.

From the densities at 20° and 30° C, fairly good values of the volume coefficients of expansion can be calculated for 25° C. These volume or density coefficients,

$$\frac{1}{V}\left(\frac{dV}{dT}\right) \quad \text{or} \quad -\frac{1}{\rho}\left(\frac{d\rho}{dT}\right)$$

per degree centigrade, are shown in column 5 of table 1. The average value for the eight samples of latex, A through H, is 0.00041/deg C. It can be seen that the dilution of a latex (sample 0.5H) greatly decreases this coefficient.

In a manner somewhat similar to the dependency of the density of a latex on its DRC, the volume coefficient of expansion should also be dependent on the DRC. In applying this assumption, however, one must know the coefficient for serum and for rubber. The value for rubber, as previously mentioned, is known to be 0.000658/deg C, but that for the serum has never been measured. As an approximation to the correct value, the coefficient of water, 0.00025/deg, will be used here. Assuming sample 37 to contain 37 percent DRC and 63 percent water, its coefficient is calculated to be 0.00040, which is in good agreement with the average of those measured. It can be seen from the lack of order of the values of the coefficients in column 5 of table 1 that this measurement is not sufficiently precise to allow a calculation of even an approximate value for the DRC. However, it may be of value to determine whether a latex sample is naturally low in DRC or whether it has been greatly diluted with water. This condition of the latex could probably better be determined from DRC and density measurements.

Figure 3 shows the relation between the density of a sample of latex and its DRC calculated from the equation previously given. The points represent experimental values obtained in this investigation for the various samples of mangabeira latex. Table 1, column 6, gives the DRC

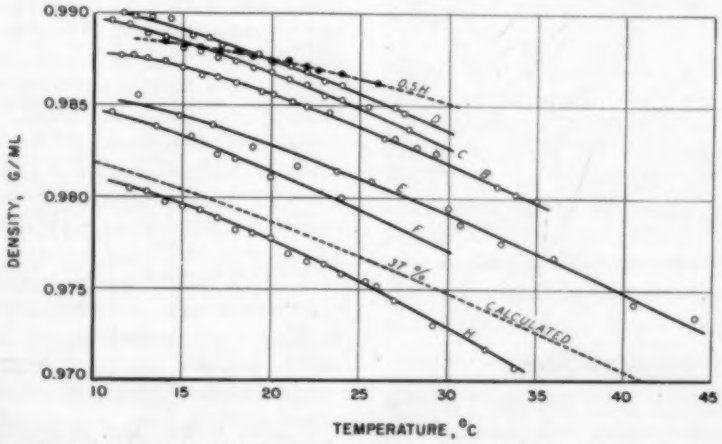

FIGURE 2.—*Density values of different samples of mangabeira latex at various temperatures.*

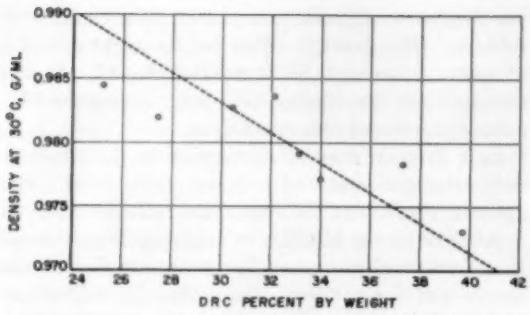

FIGURE 3.—*Dry rubber content of latices as a function of the density.*

The dotted curve is plotted from data of Rhodes [11] for Hevea latex. The points are experimental values obtained for mangabeira latex in the present investigation.

of the latices as calculated from the densities. These values are to be compared with those determined by coagulation in the adjoining column to the right. It can be seen from figure 3 that the deviation of some of the points from the curve is quite great, but for approximate values of DRC the formula given for the latex of Hevea also can be applied to that of mangabeira.

It will be noted from the table that the true DRC and the density-calculated DRC for latex H are in good agreement with each other, but when this latex is diluted 1:1 with water (sample 0.5H) its density-calculated DRC is much too high. This is because of the high density of the serum. In fact, pure water is calculated from the formula to have a DRC of 19.5 percent. Sample 37 is plotted in figure 2 from calculated values of the density at 30° C for a latex with 37 percent DRC. Values for the curve at other temperatures are calculated by using the coefficients of expansion of the rubber and water in their proper proportion for these other temperatures. The coefficient for rubber is practically constant over this range of temperature for purposes of this calculation, but the coefficient for the water changes so rapidly, especially at the lower temperatures, that the resulting curves for the latices are not linear. The shapes of all the experimental curves are very similar to that of the theoretically calculated curve 37.

3. Coagulating Agents

As stated earlier in this paper there are a number of coagulating agents which will separate the mangabeira rubber from its serum, but only a few of these agents have any commercial possibilities. Acetic acid, for example, which is used in a concentration of less than 1 percent (commercial grade) for the coagulation of latex from the seringueira or Pará tree, must be added in much larger quantities in order to coagulate mangabeira latex. As shown in table 2, a concentration of 5 ml of glacial acetic acid per 100 ml of latex is not sufficient for coagulation. Usually twice this concentration is sufficient if the latex has had no previous dilution. However, this is not always true, as in some cases at least 25 ml per 100 were necessary. There is some variability between different latices, but the data given in table 2 are typical and close to average. Complete coagulation can correctly be assumed if the resulting serum is not milky in appearance. Even a very small amount of rubber left in serum causes it to be noticeably milky. Coagulations with acetic acid, when they do take place, are quite rapid, requiring usually 15 to 20 minutes or less. Acetic acid coagulations give satisfactory results as a laboratory procedure for analysis of the DRC of mangaberia latex, but too much of this acid is required for industrial processing.

TABLE 2.—*Results obtained from various coagulating agents on mangabeira latex*

Coagulant		Water added to 100 ml of latex	Serum condition	Time required for complete coagulation
Type	Added to 100 ml of latex			
	ml	*ml*		*Minutes*
Glacial acetic acid	5	0	Quite milky	
Do	10	0	Clear	2
Do	10	100	Quite milky	
Do	10	200	Very milky	
Do	20	0	Clear	2
Do	20	100	Somewhat milky	
Do	20	200	Quite milky	
Do	30	0	Clear	1
Do	30	100	Slightly milky	
Do	30	200	do	
Caxinguba latex	2	100	Somewhat milky	
Do	4	100	Clear	6
Do	8	100	do	2
Hydrochloric acid	0.1	100	Somewhat milky	
Do	.25	100	Clear	60
Do	.5	100	do	5
Do	1	100	do	1
Do	2	100	do	1
Do	4	100	do	1

It was found that hydrochloric and sulfuric acids in much smaller quantities coagulate manga-

beira rubber equally well or even better. This can also be seen from table 2. The degree of dilution of the latex does not have much effect on the quantity of acid required for coagulation. If there is no dilution and 10 or 20 ml or more of concentrated hydrochloric acid are added, the rubber will coagulate completely, but the physical characteristics of the rubber are changed. For example, the rubber will crumble into small pieces when passed through a mixing mill and will have a slight pungent odor. However, small concentrations of the acid produce a rubber of good quality.

As can be seen from table 2, the concentration of the acid in the latex has a great effect on the time of coagulation. Although, for the particular sample of latex described in the table, 0.25 percent of commercial hydrochloric acid in the latex was sufficient for complete coagulation, experience has shown that it is safer to add 0.5 percent. For the factory coagulations conducted in connection with this work, 1 liter of water was first added to a liter of the latex, and then 5 ml of the concentrated acid in 50 ml of water were added. This produced a satisfactory coagulum, which was ready for rolling into sheet form in about 12 hours.

If the latex is not diluted before coagulation, or if the coagulation takes place in too short a time, the resulting coagulum is not as uniform and is much harder, thus making the sheeting process more difficult. Undiluted latex with a high DRC does not leave sufficient liquid for the coagulum to float, and the spongy solid phase, together with its absorbed serum, occupies the whole space from the surface of the coagulum to the bottom of the container and often sticks to the bottom. If the dilution is too great, or if too long a time is required for coagulation, the resulting coagulum is too weak for proper handling during the sheeting process. Complete coagulation within a few hours seems to give the most satisfactory product. After complete coagulation, it is advisable also to allow several hours for the coagulum to harden sufficiently. The proper amount of dilution allows the coagulum to form more slowly and uniformly and also to float on the surface of the liquid, thus facilitating the removal of the rubber phase. This makes the processing operation convenient for tapping and collection in the morning, addition of the coagulating agent in the early afternoon, and sheeting in the late afternoon or following morning.

Latex from the caxinguba tree (*Ficus anthelmintica*) acts as a coagulating agent for the latex of mangabeira.[4] The caxinguba tree is found in the tropics of Brazil, in no great concentration in any one area, but quite widely distributed. Its latex can be recommended as an excellent coagulant for the latex of the mangabeira if the two trees are found in the same area. A lack of rapid and dependable transportation in the rubber-growing areas may prevent the relatively unstable caxinguba latex from being transported over any great distances. The latex to be coagulated can be diluted 1:1 with water, and the caxinguba latex added either in its original or diluted state. About 5 percent concentration of latex is recommended, or about 50 ml per liter of mangabeira latex. Incidentally, the latex of the caxinguba is also a very good coagulant for the latex of the Hevea, a much lower concentration of the coagulant being required than for mangabeira.

Alum solutions and sodium chloride solutions have been the coagulating agents used by the natives in the production of the mangabeira rubber. These salts were studied as coagulants in this investigation by adding them as 10-percent solutions. Both coagulants gave a nice looking coagulum that sheeted easily. The amount of coagulating agent usually used to insure complete coagulation was about 100 ml of the 10-percent solution per liter of the latex.

As stated earlier in this paper, partial coagulation of the rubber from mangabeira latex may take place from agitation, even though it is quite mild like that taking place in most laboratory stirring operations. In attempts made to concentrate the latex by means of a centrifuge, coagulation always took place. Guimaraes and Chaves [3] reported that their mangabeira latex could be coagulated by means of vigorous agitation. It seems quite probable that a successful commercial coagulation method may be developed based on this principle.

4. Chemical Composition of the Rubber

Not all the samples of rubber were analyzed, but table 3 shows the averages of the results

[4] Hugo Borborema, under the supervision of Felisberto C. de Camargo, director of the Instituto Agronômico do Norte, found that the latex of caxinguba was effective as a coagulant for the latex of mangabeira. Their experiments were conducted at the latex-processing factory of the Instituto Agronômico do Norte, and further study of this method of coagulation was turned over to the Rubber Laboratory.

obtained. The resin content of the mangabeira rubber, which in most cases runs from 10 to 13 percent, is higher than that for the Hevea rubber, which is usually below 4 or 5 percent. The resin content is higher for a rubber prepared from latex by evaporation. This indicates that in ordinary coagulation some of the resins remain in the serum.

TABLE 3.—*Results of analyses on dry coagulated mangabeira rubber*

Sample	Resins	Ash
	Percent	*Percent*
B	[a]10.6	0.17
C	11.5	.20
D	13.3	.17
G	7.3	.29
H	6.7	.....
I	12.8	.14
J	[b]9.3	.13

[a] 13.0% resins on a sample of evaporated latex.
[b] 13.4% resins on a sample of evaporated latex.

In the five samples for which determinations of both DRC and resins were made there is indicated a trend that latices having a higher DRC yield a rubber of lower resin content. Whether or not this is generally true must be proved by similar analyses on many more samples of latex.

The ash content of mangabeira rubber (table 3) averages 0.2 percent, which is about the same as that usually found in Pará rubber. In a few instances, however, when the mangabeira rubber was coagulated by means of sodium chloride, the ash content was higher (0.4 to 0.6%). This should be expected because of the difficulty of washing out completely the coagulant from the coagulum. No doubt an alum coagulation leaves an equivalent amount of alum in the rubber, but this does not show up so strongly in the ash because over 70 percent of the absorbed alum is lost during the ignition process. More detailed analyses on mangabeira latex and rubber were made by Guimaraes and Chaves and published earlier [3].

5. Physical Properties of the Rubber

In order to evaluate the mangabeira rubber, especially as to its aging properties, tensile tests were made on both aged and unaged vulcanized samples. Samples of the mangabeira rubber coagulated by different means were also tested and compared with a typical sample of Hevea rubber.

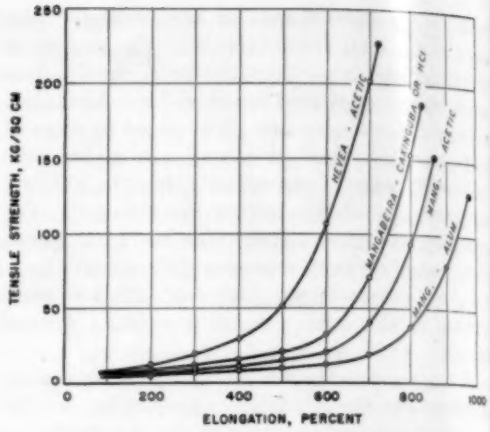

FIGURE 4.—*Tensile properties of vulcanized Hevea rubber coagulated with acetic acid compared with mangabeira rubber coagulated by different agents.*

Figure 4, which contains curves made from average values obtained from a number of tests and samples, shows that the Pará rubber has higher tensile properties than the mangabeira. The mangabeira rubber coagulated with caxinguba latex or with dilute hydrochloric acid gives tensile properties superior to those of samples coagulated with acetic acid or alum. The alum-coagulated rubber has the poorest properties of all. Actually, this evaluation may quite easily have been indicated without vulcanizing the rubber and determining its tensile properties. Rubber coagulated with alum is somewhat tacky and becomes much more so within several weeks time. The rubber coagulated with acetic acid is also tacky, but to a less degree. The rubber coagulated with the latex of caxinguba or with dilute hydrochloric acid exhibits no tackiness even over a period of a year or more.

The pinkish appearance which is characteristic of mangabeira latex is transferred to the rubber in all the processing methods described here. Mangabeira rubber can usually be distinguished from other types of rubber by this color.

Samples of unvulcanized mangabeira rubber coagulated by dilute hydrochloric acid or by caxinguba latex have been kept in the laboratory for over a year without any appreciable visual aging, as is indicated by their lack of tackiness. The other coagulants, especially the alum or the sodium chloride, cause the rubber to age quite rapidly. In less than 1 year the rubber becomes

so sticky that it seems almost worthless. No doubt it is this poor aging quality that has given the mangabeira rubber its bad reputation. Laboratory aging tests were made by means of the oxygen bomb, as previously described. The stress at break for mangabeira rubber coagulated with the caxinguba or dilute hydrochloric acid in all cases decreased no more than 50 percent during the aging process. The rubber samples coagulated with the salts became so badly oxidized and brittle that in some cases they broke in pieces when bent by hand. Usually, they were too weak to test on the Scott tensile tester. A few that had enough resistance to be tested were found to have deteriorated from 80 to 90 percent with respect to tensile properties.

The coagulated rubber was always thoroughly washed during the sheeting process, but chemical analyses of the rubber indicate that the coagulating agents used in these experiments were not removed completely. It is out of the question to expect commercial washing to be more effective than these small-scale operations in freeing the rubber from the small quantities of the coagulants or their impurities, which are probably the cause of the poor aging qualities of the mangabeira rubber.

V. Summary and Conclusions

1. Of a number of samples of latex of mangabeira investigated, the DRC values ranged from 25 percent to 40 percent, the average being about 33 percent.

2. A rough value of the DRC of mangabeira latex can be obtained by measuring its density and applying the same tables which are used for latex of the seringuira or Pará rubber-tree, assuming the law of mixtures on a volume basis, the density of the serum as 1.020, and the density of the disperse phase as 0.9064 g/ml at 30° C.

3. The volume coefficient of expansion for the average mangabeira latex, which contains from 30 to 40 percent DRC, is about 0.00041/°C.

4. Both for laboratory analyses for the DRC and for the commercial coagulation of mangabeira latex the best coagulants are either dilute hydrochloric acid (about 0.5%) or the latex of the caxinguba (about 5%).

5. Alum and sodium chloride solutions, both of which at the present time are used as coagulating agents in the commercial production of mangabeira rubber, have a degrading effect on the resulting product, both unvulcanized and vulcanized.

6. The resin content of the mangabeira rubber is usually from 7 to 13 percent, most values being closer to the latter. The ash content is usually quite low, about 0.2 percent.

7. The optimum conditions for vulcanization of mangabeira rubber, as determined by the highest tensile strength, are from 60 to 90 minutes at 141° C when compounded according to formula II of the Crude Rubber Committee of the Rubber Division of the American Chemical Society.

8. Mangabeira rubber is softer and weaker than Hevea rubber, but with the improved methods of processing, the physical and aging properties of the mangabeira rubber have been greatly improved, and this rubber may find commercial applications in the future, especially as a special-purpose rubber.

9. There are possibilities that still another method of coagulating rubber from mangabeira latex, making use of vigorous agitation, may be developed.

VI. References

[1] E. G. Holt, private communication.

[2] A. W. J. Dyck, private communication.

[3] L. R. Guimarães and J. M. Chaves, Coagulation of the latex of Mangabeira. Rev. brasil. quim. (São Paulo) **18,** 130 (1944).

[4] A. S. T. M. Standards, 1942. Part III, American Society for Testing Materials, 1916 Race St., Philadelphia 3, Pa.

[5] Report of the Crude-Rubber Committee, Rubber Chem. Tech. **17,** 529 (1944).

[6] O. deVries, Estate rubber: Its preparation, properties, and testing, p. 38 to 42, 111 to 121 (Drukkerijen Ruygrok & Co., Batavia, 1920).

[7] E. A. Hauser and W. J. Kelly, Latex: Its occurrence, collection, properties, and technical applications, p. 68, 70, 71 (The Chemical Catalog Co., New York, N. Y., 1930).

[8] P. Scholz and K. Klotz, Contributions to the chemistry of latex, Kautschuk **7,** 142 (1931).

[9] E. Rhodes, The specific gravity of preserved latex, J. Rubber Research Inst. Malaya **5,** 234 (1934); Rubber Chem. Tech. **8,** 284 (1935).

[10] O. deVries, The specific gravity of rubber in latex, India-Rubber J. **89,** 343 (1935).

[11] E. Rhodes, The specific gravity of preserved latex, India-Rubber J. **89,** 397 (1935).

[12] H. P. Stevens and son, Specific gravity of rubber in latex, India-Rubber J. **87,** 400 (1935).

[13] E. Schmidt and P. Stamberger, Some properties of rubber latex, Rec. Commun. Congr. Int. Caoutchouc, Paris, p. 42 (1937).
[14] N. Bekkedahl and L. A. Wood, Crystallization of vulcanized rubber, Ind. Eng. Chem. **33,** 381 (1941); Rubber Chem. Tech. **14,** 347 (1941).
[15] H. L. Curtis, A. T. McPherson, and A. H. Scott, Density and electrical properties of the system, rubber-sulfur, NBS Scientific Papers **22,** 383 (1927) S560.
[16] L. A. Wood, Values of the physical constants of rubber, Proc. Rubber Tech. Conf. London, England, p. 933 (1938); Rubber Chem. Tech. **12,** 130 (1939).
H. Fairfield Smith, Specific gravity of latex and rubber, J. Rubber Research Inst. Malaya **9,** 218 (1940); Rubber Chem. Tech. **13,** 485 (1940).
G. E. van Gils, The specific gravity of rubber and of serum in Hevea latex, Arch. Rubbercultuur **23,** 130 (1939); Rubber Chem. Tech. **13,** 422 (1940).
O. deVries, The specific gravity of rubber in latex, India Rubber J. **98,** 422 (1939); Rubber Chem. Tech. **13,** 130 (1940).

WASHINGTON, November 1, 1946

U. S. Department of Commerce
National Bureau of Standards

Research Paper RP1786
Volume 38, April 1947

Part of the Journal of Research of the National Bureau of Standards

Spectrographic Determination of Minor Elements in Portland Cement[1]

By Armin W. Helz * and Bourdon F. Scribner

A rapid spectrographic procedure for the determination of the minor metallic elements in portland cement is described. The method shows promise of easy extension to cement raw materials and many ceramic materials, provided reliable standard samples of these materials are available.

In the application of the method to portland cement, seven minor elements were determined. The precision in terms of probable error of a single determination is within 3 percent of the oxide concentration for aluminum, iron, magnesium, manganese, and titanium; 5 percent of the Na_2O concentration; and 8 percent of the K_2O concentration. Other minor elements, such as lithium, strontium, chromium, zirconium, and vanadium, may readily be included.

The spectrographic analyses of 21 portland cements are compared with chemical results for an estimate of the accuracy. Salient features of the procedure are (1) employing pellets consisting of the cement powder, with graphite as a binder, cobalt oxide as an internal standard, and potassium nitrate as a buffer, (2) applying the pellet as an electrode for excitation by an overdamped condenser discharge, and (3) photographing the spectrum with a step sector and a diffusing screen for obtaining uniformity of illumination.

I. Introduction

Portland cement is composed of several complex compounds of lime, alumina, silica, and iron oxide. Its approximate oxide composition is given in table 1. The usual chemical procedures for the analysis of cement are difficult and time-consuming. Unless special care is exercised in chemical separations, errors arise owing to interferences, thus TiO_2 and P_2O_5 may be included with Al_2O_3; Mn_2O_3 with MgO; and if minor alkali elements are present, Li_2O with Na_2O; and Cs_2O and Rb_2O with K_2O. The spectrographic method offers marked advantages of speed, ease of execution, and relative freedom from personal error.

TABLE 1.—*Composition of portland cement*

[Range and average of 41 commercial cements]

Constituent	Range	Average
	Percent	*Percent*
CaO	59.6 to 67.0	63.6
SiO_2	20.0 to 27.5	22.3
Al_2O_3	2.0 to 6.3	4.7
Fe_2O_3	1.9 to 5.5	3.4
MgO	0.7 to 4.4	2.1
SO_3	1.3 to 2.3	1.8
Na_2O	0.03 to 1.2	0.25
K_2O	.04 to 1.4	.45
P_2O_5	.03 to .46	.14
Mn_2O_3	.03 to .50	.18
TiO_2	.10 to .30	.22
Ignition loss	.60 to 2.2	1.0
Insoluble residue	1.02 to .40	0.14

The intial application of the spectrograph to the analysis of portland cement by the Bureau's spectrochemical laboratory was made on the de-

[1] Presented at the meeting of the American Ceramic Society on April 30, 1946.

* Research Associate at the National Bureau of Standards, representing the Portland Cement Association.

termination of the alkali elements [1].[2] The fullest advantage of a spectrographic method is realized when a number of elements are determined simultaneously. Consequently, an investigation was undertaken to extend the determinations to include aluminum, iron, magnesium, manganese, and titanium. At the same time the possibility of applying a modified technic to improve the alkali determinations was considered.

In the method previously reported for the alkalis, a fixed amount of the sample mixture was placed in the crater of a graphite electrode that formed the lower positive element of direct-current arc. This method has the advantages of employing the relatively inexpensive direct-current type of excitation and providing for the detection of very low concentrations. The disadvantages of the method are (1) the requirement of red-sensitive plates that tend to be nonuniform, (2) the difficulty of handling small samples in powder form, and (3) the requirement of additional procedures for lithium and for high potassium concentrations. The procedure to be described has none of these disadvantages and permits the determination of aluminum, iron, magnesium, potassium, sodium, manganese, and titanium. In addition, lithium, strontium, chromium, zirconium, and vanadium were considered, but they were not found in any of the cements analyzed in sufficient quantities to warrant their detailed study. Lines of these elements suitable for observing concentrations down to about 0.1 percent are found in the same spectral region used for the other elements. Calcium, silicon, sulfur, and phosphorus are not determined by this method. The first two elements, because of their high concentration, cannot be determined with sufficient precision to rival chemical methods. The latter two elements have poor spectral sensitivity, and special procedures would be required for their determination. The method shows promise of easy extension to the analysis of cement raw materials and many ceramic materials, if reliable standard samples of these materials are available.

II. Development of the Method

1. Spectrographic Studies

In the paper on the determination of the alkalies in portland cement [1] the K 7698.98 and Na 8194.81 A lines were used in preference to K 4044.14 A and Na 3302.32 A because of the higher intensity and greater freedom from background. The shorter wavelength potassium and sodium lines are much more useful because of their proximity in wavelength to lines of other minor elements. The procedure described in this paper successfully makes use of the K 4044.14 and Na 3302.32 A lines through the choice of excitation and the form and composition of the electrode. The potassium line tends to be broad and diffuse. This, however, does not seriously impair its usefulness for quantitative work.

There was no difficulty in finding suitable iron, magnesium, and titanium arc lines. Their selection was based on consideration of intensity, proximity to other lines being measured, and freedom from interfering lines. Limitations of intensity and background narrowed the choice of magnesium lines. The Mg 3332.13 A line was successfully used, though it tends to be weak and diffuse. Attempts were made to use an aluminum line falling within the region 2800 to 4200 A photographed for the other elements. Aluminum lines in this region were either too intense or failed to show a favorable intensity-concentration response. For this reason the Al 2660.39 A line was selected. A coincident line, Fe 2660.40 A, did not interfere with the aluminum line at the concentrations of iron encountered in cements. The weaker line, Al 2652.49 A, is suggested as an alternate for the determination of aluminum.

The spectrum was photographed with a Bair grating spectrograph having a linear dispersion of approximately 5.5 A per millimeter. An intensity pattern is obtained with a five-step rotating sector and a thin silica lens, the combination being located at the secondary focus of the spectrograph. The lens serves to focus an image of the arc on the grating of the spectrograph. This arrangement is not sufficient for obtaining uniform illumination as the arc is very large and the distribution of the intensities of the lines of the several elements varies at different points in the arc. This is particularly true of the alkali lines as compared with those of the internal standard and the other elements sought. This difficulty is minimized by placing a diffusing screen at the position where the arc would normally be and moving the arc to a position 8 cm behind the screen.

[2] Figures in brackets indicate the literature references at the end of this paper.

The arc stand has been described by Scribner and Corliss [2]. The adapter (fig. 1) used to hold ¼-in.-diameter pellet electrodes in this stand will also serve with any other electrode holder that will clamp rods ¼ in. in diameter in accurate alinement. The clamping action of the stand on the split rod of the adapter securely clamps the sides of the pellet. The pellet extends well above the rim of the adapter so that the arc strikes only the top face of the pellet. With proper clamping, the bottom of the pellet and the adapter remain perfectly clean and free from burning.

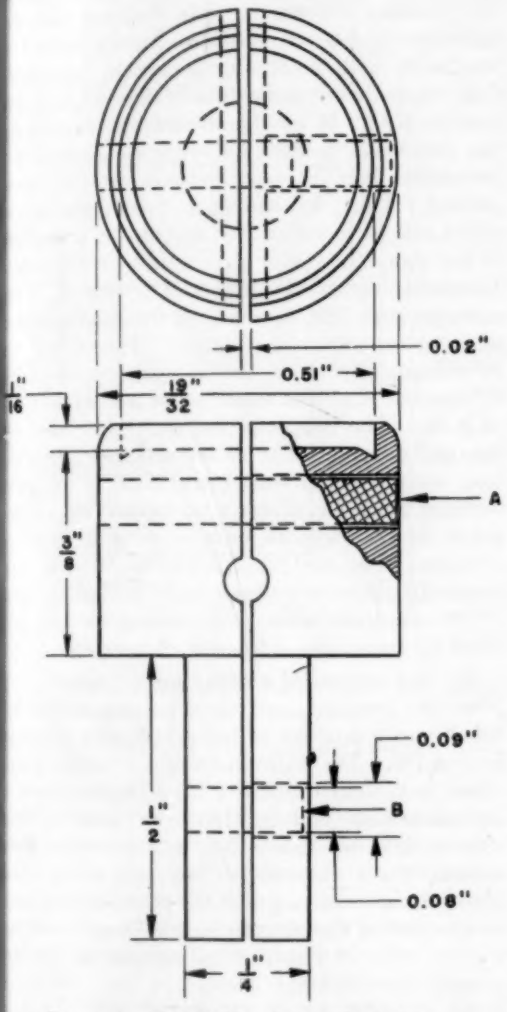

FIGURE 1.—*Pellet holder, front and top views.*

It is made by turning two pieces of brass clamped together with a metal spacer 0.02 in. thick. Two steel-pin guides (*A*, *B*) are soldered to the left side and extend into oversized holes in the right side.

The diffusion screen is similar to that discussed by Hansen [3] and consists of a vitreous silica plate, 45 mm in diameter, ground, and etched for maximum transmission, with good diffusion. It is made by grinding a clear silica plate on one side with grade *F* silicon carbide and then etching in dilute hydrofluoric acid for about half an hour. The etching is discontinued when inspection with magnifying lens shows that the irregular scratches of the grinding are smoothed out into hemispherical pits. Details of photography, microphotometry, and calculations follow standard procedures, and for which adequate references are available [4, 5].

2. Method of Excitation

Three means of excitation were investigated (1) direct-current arc, (2) alternating-current arc, and (3) overdamped-condenser discharge. The latter appeared more promising for a simultaneous determination of all minor elements than the other types of excitation. Tests indicated that insufficient reproducibility was obtained for the alkalis with the d-c or a-c arcs, but such arcs did show possibilities of giving satisfactory results for other minor elements.

The overdamped-condenser discharge was obtained with a "multisource unit" [6, 7]. This instrument supplies a large number of discharges intermediate between the electric arc and electric spark. The arc-like discharge was chosen because of sensitivity and interference considerations, and has the current characteristic shown in figure 2. The circuit constants given in the procedure below are optimum for reliable operation of the power unit under high-energy and high-damping requirements. The large gap is essential for stable operation and the negative polarity of the sample-bearing electrode was chosen because of enhanced spectral intensity.

3. Electrode Form, Composition, and Preparation

Numerous tests showed that improved reproducibility could be obtained with the pellet method of placing the sample in the arc, furthermore, the spectral background was considerably reduced. The pellets are disk-shaped ½ in. (13 mm) in diameter and ⅛ in. (3 mm) thick.

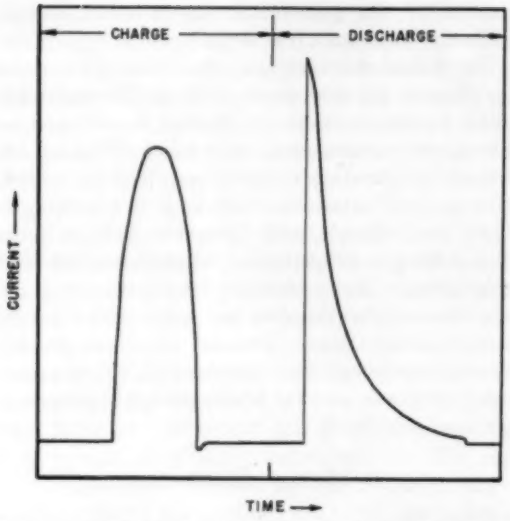

FIGURE 2.—*Sketch of oscillogram of overdamped-condenser discharge, showing the change of current with time for charge and discharge of the condenser.*

Second-grade spectroscopic rods ⅛ in. in diameter cut into electrodes ¾ in. (19 mm) in length and rounded at one end served as the upper, positive, electrode.

Graphite proved to be an ideal admixture with the cement for obtaining a pellet which, upon burning, was slow to form a crust. With this type of pellet a constant ratio of intensities of lines of the various elements is maintained for a fairly long burning time. The concentration of cement was made as high as possible in order to obtain suitable intensities of the desired lines (particularly for the alkalis). The upper limit was found to be about 60 percent cement, which, if exceeded, produced erratic burning and crust formation.

Cobalt oxide is added for the internal standard. Cobalt has a sufficient number of lines to provide suitable reference lines in any part of the spectrum, and has evaporation and excitation characteristics that are a fairly good average of the properties of the elements sought. The purest compound of cobalt available was $Co(NO_3)_2.6H_2O$, from which the oxide was prepared.[3]

An important problem was the effect of varying potassium content on the intensity ratio of sodium to cobalt. The spectra of other minor elements showed little alteration with respect to cobalt lines. The choice of another internal standard, strontium, for example, would prove better for sodium but poorer for the other minor elements. A single internal standard could not be ideal for all the elements in question because of differences in properties of the elements to be determined. The method and reason for reducing the potassium interference in preference to adding a second internal standard follows. It was observed that the interference due to potassium tends toward a maximum with increasing potassium concentration—there being little further change above 1.0 percent K_2O. It was found desirable to increase the potassium content in order to increase the potassium line intensity relative to the background. Thus, by adding a known amount of potassium as a buffer, the amount of potassium in the sample could be determined by difference. Increasing the total amount of potassium, however, decreases the accuracy of the determination of the potassium in the sample. The addition of potassium nitrate to the sample equivalent to 0.7 percent K_2O was found to be a suitable compromise. The nature of the compound used for this addition proved to be important. The addition of potassium carbonate resulted in poor burning behavior whereas potassium nitrate resulted in very smooth burning with all types of cements. The arc under these conditions continuously played over the central half of the area of the electrode without remaining at any one point for more than a fraction of a second.

The ingredients of a pellet are (1) cement, (2) powdered graphite, and (3) a potassium nitrate-cobalt oxide mixture in the proportions given in section III. The latter mixture is prepared in advance in sufficient quantity for a large number of determinations and is mixed by grinding and sieving, first through a No. 325 sieve and then several times through a No. 200 sieve. The above three constituents of the pellet are weighed as specified in the procedure, mixed, and used for a single pellet. The final mixing may be done by passing the material through a No. 100 sieve three or more times. However, the following procedure for mixing is faster, with less chance of introducing errors. A number of vials are pre-

[3] Cobalt oxide was prepared by carefully heating the nitrate in a Pyrex beaker to remove water and oxides of nitrogen. The product was crushed and passed through a No. 48 sieve and then transferred to a platinum dish and heated to about 900°C for several hours. Finally, the oxide was passed through a No. 200 sieve.

pared, each one to hold a sample mixture.[4] A vial containing the ingredients of a pellet is placed in a plastic holder, shown in figure 3, and clamped to an electric-motor shaker for mixing. The clamp is designed to press the cover [5] against the vial and to hold the entire assembly in place. A dental-type amalgamator shakes the vial in a figure-8 motion at high speed. Twenty seconds of shaking

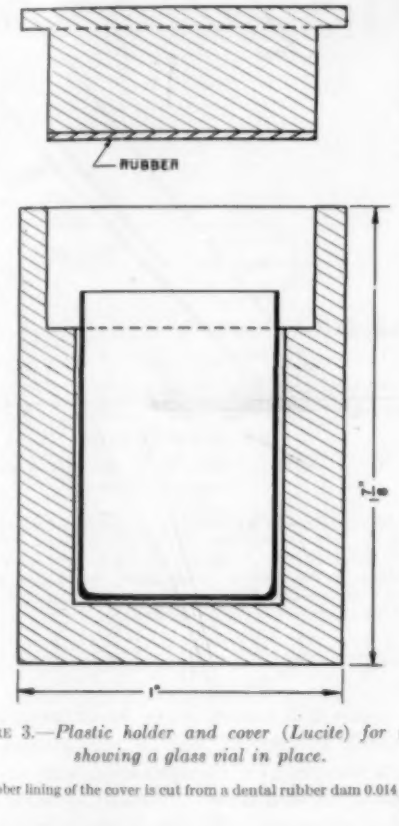

FIGURE 3.—*Plastic holder and cover (Lucite) for mixing, showing a glass vial in place.*

The rubber lining of the cover is cut from a dental rubber dam 0.014 in. thick.

is sufficient for complete mixing. A number of sample mixtures are prepared simultaneously. When making a pellet the complete contents of a vial is poured into the mold. Sufficient pressure is applied in the press to give a well-formed, compact pellet capable of easy handling.

[4] The vials are prepared by cutting off thin glass vials 5/8 in. (16 mm) in diameter, and grinding, and polishing the open ends to a total length of 1 5/8 in. (41 mm).

[5] A thin rubber sheet cemented to the cover of the holder and pressed against the ground and polished ends of the vials efficiently retains the material during mixing.

III. Procedure

The following three materials are weighed into a glass vial for mixing: (1) Spectrographic graphite powder (note 1, table 2) 0.440 g; (2) potassium nitrate–cobalt oxide mixture, 0.0575 g; (3) portland-cement sample, 0.500 g. Mixture 2 is prepared with 5.000 g of cobalt oxide and 0.750 g of potassium nitrate, as already described. If the cement has been stored for a considerable time or exposed to air, it should be ignited at 900° C and passed through a No. 100 sieve. Pellets are formed in a mold ½ in. in diameter at a total load of about 8,500 pounds. The value of the pressure is not critical, except that it should be kept constant. Any burrs on the pellet are scraped off and the pellet brushed clean, all handling being done with forceps. Details for making the spectrogram are outlined in table 2.

TABLE 2.—*Operating conditions for analysis of portland cement*

1. Upper electrode	Graphite rod, ¼ in. in diameter by ¾ in. long, rounded at one end.
2. Lower electrode	Cylindrical pellet ½ in. in diameter, representing the prepared sample mixture, polarity negative (note 2).
3. Gap	8-mm initial setting, unaltered during exposure.
4. Alinement	Top of pellet 3 mm below the optic axis.
5. Optics in front of slit	Light passes from the arc 8 cm to diffusing screen, thence 40 cm to illuminating lens (f_D=44 cm), thence 1.5 cm to rotating step sector, and finally 10 cm to slit.
6. Power	Multisource unit, overdamped condenser discharge (note 3).
a. Capacitance	45 μf.
b. Inductance	400 μh.
c. Resistance	40 ohms.
d. Phase angle	30 degrees.
e. Output potential	940 v.
f. Input current	2.4 A.
7. Exposure time	45 seconds.
8. Spectrograph	Grating, Eagle mounting. 5.5 A/mm.
a. Grating aperture	Full opening of grating used.
b. Slit width	50 μ.
c. Region	4200 to 2900 A, and 3500 to 2200 A.
9. Photographic plate	Eastman Spectrum Analysis No. 1.
10. Development	2.5 minutes, 21°C, Eastman formula D-19, continuous agitation.

NOTE 1.—A pure form of graphite powder suitable for forming the pellets was obtained from the National Carbon Co.

NOTE 2.—One side of the pellet may be used for the aluminum determination and the other side for the other elements when the apparatus will not permit covering the entire region (4,100 to 2,600A) with a single exposure.

NOTE 3.—Before running samples for analysis, the source unit must be warmed-up by running several blanks.

Reduction of measurements follows standard procedures. Intensities of the lines of the elements sought relative to the intensities of neighboring

cobalt lines are derived from plate characteristic curves (transmittancy vs. log relative intensity) established for each of the first three groups of lines indicated in table 3. The log intensity ratios are converted to concentrations of the elements by means of analytical curves. The latter are determined by applying the same spectrographic procedure to portland cements of known composition. The majority of photometric measurements are made in the second and third steps of the intensity pattern. The Li, Cr, Sr, V, and Zr lines listed in table 3 are for qualitative observation. These elements were not found in appreciable amounts in any of the 41 cements studied. Therefore, the lines were not tested for quantitative work but are of an intensity suitable for detecting oxide concentrations in the neighborhood of 0.05 percent. A weak cobalt line tends to interfere with the lithium line, but lithium can be detected in amounts as low as 0.1 percent of Li_2O.

TABLE 3.—*Lines employed in the analysis of portland cement*

[Wavelengths in angstroms]

Element	Analytical line	Internal standard (cobalt lines)	Concentration range (as oxide)	Index [a]
			Percent	*Percent*
K	4044.14	4020.90	0.04 to 1.4	1.3
Mn	4041.37	4020.90	.03 to 0.50	0.15
Fe	4005.25	4020.90	1.9 to 5.5	2.6
Ti	3998.64	4020.90	0.10 to 0.30	0.18
Mg	3332.15	3322.20	.70 to 4.4	3.4
Na	3302.32	3322.20	.03 to 1.2	0.34
Al	2660.39	2648.64	2.0 to 6.3	4.4
Li	3232.61	.....	.....	.....
Cr	3578.69	.....	.....	.....
Sr	3464.46	.....	.....	.....
V	3183.41	.....	.....	.....
Zr	3391.97	.....	.....	.....

[a] The index is the concentration for which the intensities of the analytical line and the internal standard line are equal.

IV. Results and Discussion

1. Analytical Curves

Figure 4 illustrates the analytical curves as determined from the reference series of 20 cements discussed in section IV, 3. The curves are not directly applicable in another laboratory because they are a function of the particular spectrographic installation. All the analytical curves are straight lines, except that for aluminum. An auxiliary scale, shown for the potassium curve, automatically deducts the 0.7 percent of K_2O added to the sample.

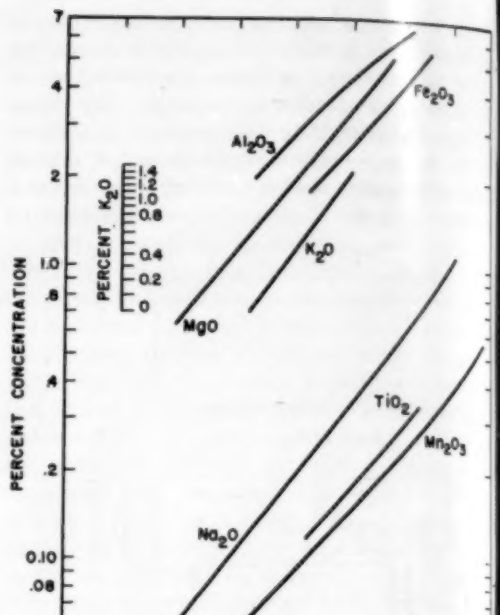

FIGURE 4.—*Analytical curves for the analysis of portland cement.*

The log intensity ratio and the percentage concentration are plotted for the following line pairs: K 4044.14/Co 4020.90; Mn 4041.37/Co 4020.90; Fe 4005.25/Co 4020.90; Ti 3998.64/Co 4020.90; Mg 3332.15/Co 3322.20; Na 3302.32/Co 3322.20; Al 2660.39/Co 2648.64. The auxiliary concentration scale for potassium oxide corrects for potassium added to the sample. The analytical curves are shown for illustrative purposes only.

The analytical curves have been found to be quite stable in general, but an unexplained shift has been observed for the potassium curve. This shift has occurred after an interruption in the work for about a month. This indicates the advisability of periodic check-ups on the potassium determination with standard samples.

2. Precision of Determinations

Estimates of precision were based on 6 determinations of the minor elements in 8 portland cements, or 48 determinations in all. The precision is an indication of the degree of reproducibility but does not indicate constant errors due to such factors as chemical combinations of the minor elements, varying composition of the major

lements, interfering elements, self-reversal, etc. Good precision, however, is a necessary condition for accuracy. In the second column of table 4, estimates of precision in terms of percentage concentration of the component are given.

TABLE 4.—*Precision and accuracy of determinations of constituents in portland cement*

Component	Precision [1] (probable error (%) of a single determination)	Accuracy [2] (average concentration difference (%) of sample)
Al_2O_3	3	0.25
Fe_2O_3	2	.12
MgO	3	.14
Na_2O	5	.02
K_2O	8	.06
Mn_2O_3	3	.01
TiO_2	2	.01

[1] Based on reproducibility.
[2] Based on differences between spectrographic and chemical determinations.

The probable error of a single determination is within 3 percent of the oxide concentration for aluminum, iron, magnesium, manganese, and titanium, 5 percent of the Na_2O concentration, and 8 percent of the K_2O concentration. The larger values for the alkalis may be due to different characteristics of volatility and excitation for the alkalis and the internal standard. Ease of contamination and the necessity of adding potassium nitrate to the sample, with the subsequent problem of mixing, may also be contributing factors to decreased precision for the alkalis.

3. Accuracy of Determinations

A measure of accuracy is obtained by comparing the chemical and spectrographic results of a large number of cements. Thus, possible effects of varying composition and of interfering elements are included. Two groups of cement samples that had been carefully analyzed were available. One group of 20 cements was used for determining the analytical curves, the second group of 21 cements was analyzed as unknown. The use of analyzed cements for standards is considered a more trustworthy procedure than the use of synthesized standards. In order to avoid the effects of differences in chemical combinations, the synthesized standard mixtures would have to be

TABLE 5.—*Comparison of spectrographic and chemical results for 21 portland cements—weight percent*

No.	Al_2O_3 [a]			Fe_2O_3 [a]			MgO [a]			Na_2O			K_2O			Mn_2O_3			TiO_2		
	Spec. A	Chem. B	Chem. C	Spec. A	Chem. B	Chem. C	Spec. A	Chem. B	Chem. C	Spec. A	Chem. B	Chem. C	Spec. A	Chem. B	Chem. C	Spec. A	Chem. B	Chem. C	Spec. A	Chem. B	Chem. C
1	5.3	5.6	....	2.4	2.4	....	3.6	3.6	....	0.25	0.24	....	0.61	0.59	....	0.08	0.07	....	0.24	0.23	....
2	5.4	5.8	....	2.4	2.4	....	3.2	3.3	....	.37	.36	....	.55	.45	....	.11	.11	....	.26	.24	....
3	4.6	4.7	4.7	2.3	2.1	2.3	1.4	1.0	1.1	.04	.03	0.04	.20	.19	0.21	.10	.09	0.08	.29	.30	0.33
4	4.5	4.7	4.7	2.9	3.0	3.1	2.4	2.4	2.2	.05	.06	.07			1.4	.14	.13	.13	.23	.21	.28
												1.5	1.4								
5	5.6	5.4	....	2.6	2.5	....	.88	.71	....	.07	.06	....	.20	.19	....	.06	.07	....	.26	.27	....
6	4.9	4.7	....	3.4	3.5	....	1.9	1.9	....	.30	.28	....	.50	.49	....	.13	.13	....	.26	.26	....
7	5.4	5.4	....	3.0	3.1	....	1.07	.94	....	.08	.07	....	.44	.44	....	.17	.16	....	.30	.30	....
8	5.8	6.1	....	2.2	2.3	....	2.1	2.1	....	.14	.16	....	.02	.13	....	.50	.50	....	.23	.24	....
9	4.0	4.0	....	3.2	3.2	....	1.2	1.2	....	.31	.25	....	.59	.44	....	.08	.09	....	.24	.23	....
10	4.8	5.5	....	3.8	3.9	....	3.3	3.1	....	.28	.26	....	.40	.39	....	.06	.07	....	.31	.30	....
11	4.7	4.3	4.2	6.0	5.4	5.5	.95	.85	.71	.71	.66	.70	.31	.15	.15	.07	.07	.06	.30	.29	.36
12	4.7	4.8	4.9	4.8	4.9	4.9	2.9	2.8	2.5	.05	.05	.05	1.3	1.4	1.4	.32	.30	.29	.23	.21	.26
13	4.7	4.6	....	5.0	4.9	....	2.2	2.2	....	.26	.25	....	.55	.54	....	.05	.06	....	.27	.27	....
14	5.5	5.0	....	2.3	2.1	....	3.8	3.2	....	.28	.28	....	.25	.26	....	.09	.09	....	.21	.22	....
15	5.4	5.2	....	2.7	2.5	....	1.5	1.4	....	.29	.27	....	.56	.46	....	.07	.06	....	.27	.27	....
16	4.5	3.9	4.0	3.3	3.3	3.4	2.7	2.3	2.3	.36	.32	.28	.27	.26	.28	.22	.22	....	.22	.23	....
17	4.2	4.6	4.5	4.8	5.0	5.0	2.6	2.7	2.4	.04	.05	.05	1.1	1.3	1.3	.29	.32	.28	.21	.23	.25
18	2.8	2.8	2.9	2.6	2.7	2.8	1.6	1.7	1.8	.16	.16	.15	.17	.24	.28	.15	.17	....	.14	.16	....
19	3.6	3.7	3.5	3.1	3.1	3.2	1.2	1.0	1.4	.38	.38	.33	.04	.04	.01	.11	.11	....	.17	.19	....
20	5.1	4.9	4.7	4.7	4.5	4.8	1.4	1.5	1.6	1.09	1.17	1.04	.16	.12	.08	.10	.11	....	.24	.25	....
21	3.3	3.1	3.1	3.3	3.3	3.4	1.7	1.6	1.5	.08	.08	.08	.35	.27	.27	.09	.09	.09	.16	.19	.17

[a] Chemical values under B and C are corrected for minor oxides.

TABLE 6.—*Effect of variable operating conditions on apparent composition*

[Values in italics represent deviation from standard procedure]

Operating conditions				Apparent composition (weight percent)				Remarks
Exposure time	Output potential	Vertical distance between lower electrode and optic axis of spectrograph	Pellett-forming load	K_2O	Fe_2O_3	MgO	Na_2O	
Seconds	*v*	*mm*	*lb.*					
45	940	3	8,500	0.28	3.6	2.8	0.42	Beginning, normal.
40	940	3	8,500	.21	3.5	2.7	.43	Exposure time short.
50	940	3	8,500	.27	3.6	2.9	.42	Exposure time long.
45	*920*	3	8,500	.21	3.5	2.7	.43	Voltage low.
45	*960*	3	8,500	.28	3.5	2.8	.42	Voltage high.
45	940	*1*	8,500	.28	3.5	2.9	.44	Arc position high.
45	940	*5*	8,500	.19	3.4	2.8	.42	Arc position low.
45	940	3	*7,500*	.26	3.5	2.6	.41	Pellett-forming pressure low.
45	940	3	8,500	.24	3.4	2.8	.43	End, normal.

heated to a high temperature to produce a product comparable to cement. This operation may cause alterations in composition, so that checking by means of chemical analysis would still be required.

Table 5 gives a comparison of the spectrographic results (columns A) with chemical results (columns B and C). The spectrographic results shown are the averages of three determinations, and the chemical results are averages of three or more determinations. The chemical results represent work by three well-qualified laboratories, and are in much better agreement than the work of the usual control laboratory. Values in columns B are the results of one laboratory, and those in columns C are the results of two other laboratories (six samples by one, and four by another).

A summary of these results, in terms of the average differences between the spectrographic (A) and the chemical results of column B, is shown in the third column of table 4. The average difference between the chemical and spectrographic values for Al_2O_3 is given as 0.25 percent, whereas that for TiO_2 is 0.01 percent. Because of the differences in concentration between Al_2O_3 and TiO_2, the above values represent about the same relative accuracy, that is, 5 percent of the concentration. The average difference between the chemical and the spectrographic values for Fe_2O_3 and MgO are a little above 0.1 percent, and for the remaining oxides, except Al_2O_3 mentioned above, are well below 0.1 percent.

4. Precisions required in details of the procedure

In order to determine the care required in executing certain details of the procedure and to indicate possible sources of error, several series tests were made: (1) exposure time varied 5 seconds, (2) output potential varied 20 v, (3) vertical adjustment of the arc varied 2 mm, and (4) pellet-forming load varied 1,000 pounds. The effects these variations on the observed concentrations of K_2O, Fe_2O_3, MgO, and Na_2O are given in table 6, each result being the average of six determinations. The first and last lines give values for the normal operating conditions. The effects variations in operational details are considered very small in view of the magnitudes of the variations, which are much greater than will be encountered in routine work with reasonable care.

Nearly as great as the effect of the variations operating conditions considered above is a warm-up effect of the power unit. This may be minimized by running several blanks before starting a series of determinations and also every time the series has been interrupted for a much longer time than that required between exposures.

5. Advantages and Limitations of the Method

The chief advantage of the spectrographic method is the short time required to make the analysis. An operator can make duplicate determinations of the seven indicated minor elements in eight portland cements in a day's work and include a visual estimate of other possible minor elements under conditions not adjusted for high speed. Easy extension of the method to include additional elements is a unique characteristic. The direct use of the cement powder is a distinct advantage over methods requiring solution of the sample and chemical separations. Freedom from

rous attention to details makes personal errors ch less likely than in chemical methods or even the earlier direct-current spectrographic thod [1].

A limitation of the spectrographic method is requirement of standard samples. The compnds containing the elements sought and the ture of the major components (bulk of the mple) must be similar for knowns and unowns, unless tests are made to prove allowable eptions. The initial cost of spectrographic paratus is high. This is particularly true for present method because of the type of excition required. In view of the speed and laborving features, however, the cost per sample alyzed can be very low when large numbers of terminations are required. The type of excitan employed is similar to an interrupted directrent arc. The possibility of substituting a mpler means of producing such excitation is ggested.

V. References

[1] A. W. Helz, Spectrographic determination of sodium, potassium and lithium in portland cement with direct-current carbon arc, J. Research NBS **34,** 129 (1945) RP1633.

[2] B. F. Scribner and C. H. Corliss, An improved electrode holder for spectrographic analysis, J. Research NBS **30,** 41 (1943) RP1515.

[3] G. Hansen, Mattscheiben, Z. tech. Physik. **24,** 104 (1943).

[4] W. C. Pierce and N. H. Nachtrieb, Photometry in spectrochemical analysis, Ind. Eng. Chem., Anal. Ed. **13,** 774 (1941).

[5] W. R. Brode, Chemical spectroscopy, 2d ed. (John Wiley & Sons, Inc., New York, N. Y., 1943).

[6] M. F. Hasler and H. W. Dietert, A new spectographic source unit, J. Opt. Soc. Am. **33,** 218 (1943).

[7] M. F. Hasler and J. W. Kemp, Spectrochemical analysis of metals with the multisource unit, J. Opt. Soc. Am. **34,** 21 (1944).

Washington, May 8, 1946.